

Sponsored by



This publication by SEPM Society for Sedimentary Geology
Special Publication No. 99

***Application of the Principles Seismic Geomorphology to Continental Slope and
Base-of-slope Systems: Case Studies from Seafloor and Near-Seafloor Analogues***

and all chapters are available open access (see license terms below) through a
financial contribution from Shell.

Open Access Terms

Creative Commons license: Attribution-NonCommercial-NoDerivs 3.0 Unported

You are free:

- **to Share** — to copy, distribute and transmit the work

Under the following conditions:

- **Attribution** — You must attribute the work (but not in any way that suggests that they endorse you or your use of the work).
- **Noncommercial** — You may not use this work for commercial purposes.
- **No Derivative Works** — You may not alter, transform, or build upon this work.

With the understanding that:

- **Waiver** — Any of the above conditions can be waived if you get permission from the copyright holder.
- **Public Domain** — Where the work or any of its elements is in the public domain under applicable law, that status is in no way affected by the license.
- **Other Rights** — In no way are any of the following rights affected by the license:
 - Your fair dealing or fair use rights, or other applicable copyright exceptions and limitations;
 - The author's moral rights;
 - Rights other persons may have either in the work itself or in how the work is used, such as publicity or privacy rights.
- **Notice** — For any reuse or distribution, you must make clear to others the license terms of this work.

Full License is available at <http://creativecommons.org/licenses/by-nc-nd/3.0/>

ARCHITECTURE OF AN AGGRADATIONAL TRIBUTARY SUBMARINE-CHANNEL NETWORK ON THE CONTINENTAL SLOPE OFFSHORE BRUNEI DARUSSALAM

KYLE M. STRAUB

Department of Earth and Environmental Sciences, Tulane University, New Orleans, Louisiana 70118, U.S.A.

e-mail: kmstraub@tulane.edu

DAVID MOHRIG

Jackson School of Geosciences, The University of Texas, 1 University Station C9000, Austin, Texas 78712, U.S.A.

e-mail: mohrig@mail.utexas.edu

AND

CARLOS PIRMEZ

Shell Nigeria Exploration and Production Company, Lagos, Nigeria

email: carlos.pirmez@shell.com

ABSTRACT: The present-day continental slope offshore Brunei Darussalam (NW Borneo) displays several networks of submarine channels possessing planform attributes similar to those observed in better-studied river systems. We use shallow 3D seismic data to study one tributary network in detail. This network is located directly downslope from the shelf-edge Champion Delta and encompasses an area approximately 8 km by 24 km in the strike and dip directions. The channels in this network initiate 1–2 km down dip of the shelf edge and are not directly linked to a terrestrial river system. Mapping of shallow seismic horizons reveals that the tributary channel network is an aggradational feature constructed on top of a relatively smooth slide plane associated with a large mass-failure event. This observation highlights differences between network construction in submarine settings compared to terrestrial settings where tributary networks are net erosional features. The smooth slide plane provides us with the simplest possible initial condition for studying the deposit architecture of an aggradational submarine-channel network. An isopach map between the seafloor and the slide plane is used to unravel sedimentation trends, particularly relative rates of levee and overbank sedimentation as a function of channel relief, lateral distance from the nearest channel centerline, and distance from the shelf edge. We observe an anti-correlation between channel relief and deposit thickness, which suggests that the degree to which currents are confined within channels exerts a first-order control on local deposition rates. We also find that over 80% of the deposit volume associated with the aggradational network is within levees. Observations suggest that this channel network was constructed from turbidity currents that initiated at the shelf edge as sheet flows prior to transitioning down slope into weakly confined flows through the construction of aggradational channels. Thicknesses of channel-forming turbidity currents are estimated using the distance between channel heads and the ratio of channel to overbank deposit thickness. These two methods yield estimates for flow thicknesses that are between 1.1 and 3 times the mean relief of channels in the network.

KEYWORDS: Submarine channels, tributary networks, seismic geomorphology, levees

INTRODUCTION

Turbidity currents and the submarine channels they construct have received significant scientific attention in recent years due to their importance in shaping the morphology of continental margins (Gerber et al., 2009; Gerber et al., 2008; Kostic et al., 2002; Pirmez et al., 2000; Pirmez and Imran, 2003; Posamentier and Kolla, 2003; Pratson et al., 2007; Puig et al., 2003; Wynn et al., 2007) and because turbidite deposits on modern continental margins form major hydrocarbon reservoirs (Weimer and Link, 1991). A suite of research methods have been used to unravel the architecture of turbidite deposits and the morphodynamics associated with submarine landscapes. These methods include reduced-scale laboratory experiments (Garcia and Parker, 1993; Metivier et al., 2005; Peakall et al., 2007; Straub et al., 2008; Yu et al., 2006), numerical models (Cantero et al., 2007; Das et al., 2004; Huang et al., 2007), analysis of deposits in outcrop (Campion et al., 2000; Hodgson et al., 2006; Pyles, 2008), sediment cores (Dennielou et al., 2006; Winker and Booth, 2000), and seismic data (Abreu et al., 2003; Deptuck et al., 2003; Pirmez and Flood, 1995; Spinnelli and Field, 2001; Sylvester et al., this volume). In addition to these tools, several

recent studies of submarine environments have utilized methods developed within the geomorphology community to study terrestrial landscape evolution (Mitchell, 2005, 2006). To what degree we can transfer these tools from terrestrial to submarine environments is an area of active research.

With few exceptions (Posamentier and Walker, 2006), most studies of submarine channels have focused on systems that initiate as erosional canyons either directly connected to a present-day river system or starting at the shelf-slope break. In this paper we describe the depositional architecture of a different type of submarine system, a tributary submarine-channel network that is an aggradational feature positioned downslope of the shelf edge offshore Brunei Darussalam. The limited attention paid to net-aggradational channel networks does not correspond to their importance in continental-margin morphodynamics. Channelized stratigraphy is constructed in net-aggradational settings, and thus understanding these systems is critical for models of seascape evolution. In the marine geology community there has also been a tendency to focus on the architecture of submarine distributary networks relative to their tributary counterparts (Babonneau et al., 2002; Damuth et al., 1983; Normark et al., 1979; Vittori et al., 2000). This likely reflects an assumption, through

analogy to terrestrial systems (Crosby and Whipple, 2006; Snyder et al., 2000; Willgoose et al., 1991), that tributary networks are net-erosional features. In this paper we show that tributary networks are not always net-erosional features in the submarine environment. This study utilizes seafloor topography and imaging of the shallow subsurface stratigraphy from a three-dimensional (3D) seismic survey obtained as part of hydrocarbon exploration efforts offshore Brunei Darussalam. Our analysis and observations are centered on three questions: (1) what controls the present-day surface morphology and recent deposition trends for this aggradational tributary channel network, (2) how does the architecture of this submarine network compare to terrestrial tributary channel networks, and (3) what attributes are associated with channel initiation in net-depositional settings, particularly those located directly downslope of shelf-edge deltas?

GEOLOGICAL SETTING AND PREVIOUS WORK

The continental shelf and slope system offshore Brunei Darussalam has been the focus of several studies over the last ten years. This focus can be attributed to the availability of several generations of 3D seismic surveys which span the continental margin from the shelf to the abyssal plain. Past studies include the sequence stratigraphy of the shelf (Saller and Blake, 2003), morphology of giant submarine landslide scarps and slides (Gee et al., 2007), controls on the margin accretionary prism (Morley, 2007),

margin morphology and depositional processes (Demyttenaere et al., 2000; Hiscott, 2001; Smith, 2004; Straub and Mohrig, 2008, 2009), and scaling laws for submarine channel networks (Straub et al., 2007). Below we provide a brief summary of the geological history for this margin.

The present-day continental margin offshore northern Borneo (Fig. 1) transitioned from a compressional margin to a passive margin in the late Miocene. Since then, the morphology of the continental slope offshore Brunei Darussalam has been controlled primarily by the progradation of deltaic depocenters. Most of the sediment is delivered to the margin by three river systems, the Baram, Belait, and Tutong rivers. High sediment discharges from these rivers has resulted in the construction of a continental shelf that is 50–70 km wide and is underlain by 8–10 km of siliciclastic sediments. Using mapped seismic horizons tied to wireline logs and biostratigraphic dates, Saller and Blake (2003) estimate that the Brunei shelf edge has prograded 80 km seaward since the Middle Miocene. Beginning in the Late Miocene, progradation was highest along the northeastern part of the Brunei shelf, associated with growth of the Champion Delta. The locus of deposition shifted to the southwest during the Early Pliocene, associated with the growth of the Baram Delta. The change in deposition locus probably resulted from a capture of substantial parts of the Champion Delta hinterland drainage by the Baram River. Shelf-margin progradation during the Quaternary was relatively rapid at 11 km/My (or a total progradation of

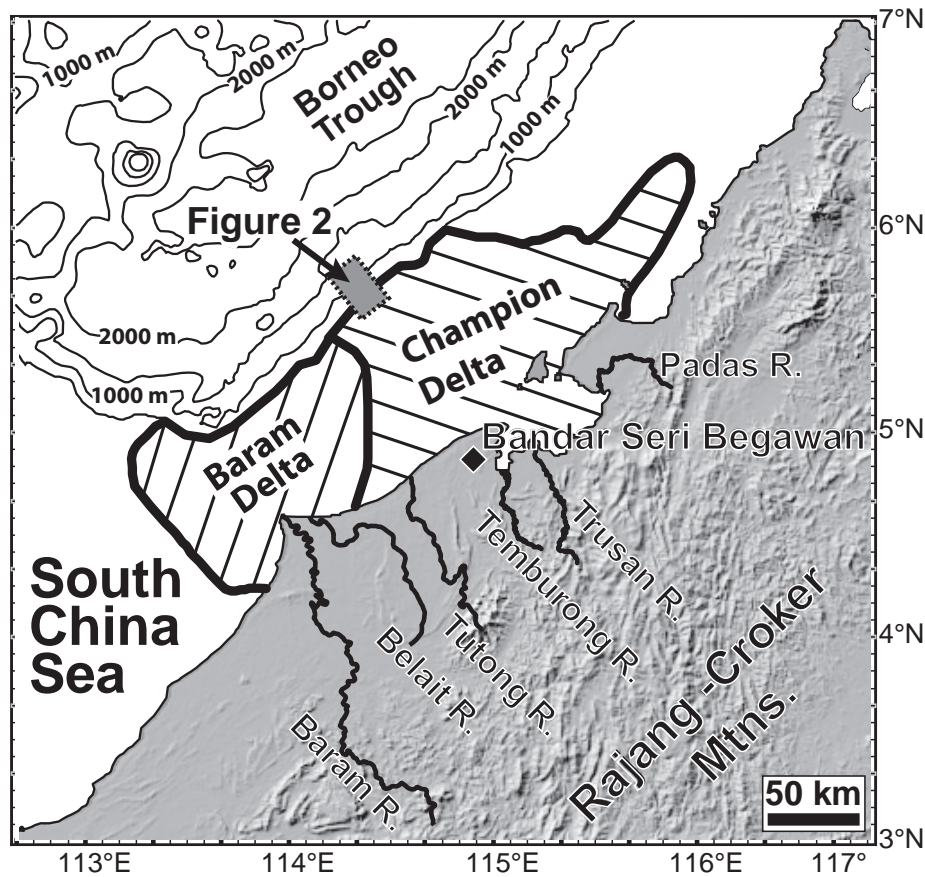


FIG. 1.—Regional topography and bathymetry map for Borneo and the South China Sea, with location of study region offshore Brunei defined by dashed box. Locations of Baram and Champion Deltas are identified in hashed regions. Boundaries defining the lateral extent of these deltas are taken from maps presented in Sandal (1996).

20 km). Quaternary deposits are thickest in the southwest associated with lowstand deltas. Of the three rivers, the Baram currently has the largest drainage-basin area and water and sediment discharges, $1.92 \times 10^4 \text{ km}^2$, $1445 \text{ m}^3/\text{s}$, and $2.4 \times 10^{10} \text{ kg/yr}$, respectively. The sediments come from the erosion of uplifted rocks in the Rajang–Crocker range in central Borneo. This mountain range is composed mainly of fine-grained mudstones and siltstones deposited in the Late Cretaceous through the Oligocene. As a result of the composition of this range and the tropical monsoon climate in central Borneo, erosion rates in this range have been amongst the highest in the world since the Eocene (Sandal, 1996).

Offshore Brunei Darussalam, the continental shelf–slope break occurs at a water depth of $\sim 180 \text{ m}$ (Fig. 2). From this position the seabed descends until reaching the floor of the Borneo Trough at a water depth of 2800 m. The upper slope is characterized by a relatively steep average gradient of 0.048 (Demyttenaere et al., 2000; McGilvery and Cook, 2003). Superimposed on this regional dipping surface are several tributary networks of submarine channels and a series of strike-parallel ridges. These ridges are the product of diapirism by mobile overpressured shale and relict fold and thrust structures. The combination of the high surface gradients, fold and thrust deformation, and shale diapirism has led to multiple mass-failure events on the upper slope (Gee et al., 2007; Steffens et al., 2003).

Exploration for and production of hydrocarbons has occurred on the Brunei continental margin for over twenty years. Numerous well penetrations demonstrate that sediments deposited on the continental margin since the Pliocene range between clay and sand, including a large fraction of deposits interpreted as turbidites. Turbidites on the continental slope of Brunei have been identified, using cores, logs, and interpretation of shallow seismic data in both relatively unconfined (Sandal, 1996) and relatively confined (i.e., channelized) (Demyttenaere et al., 2000) settings.

Seismic Data Set Parameters

The study area is 555 km^2 in area and is centered over a tributary network of channels on the continental slope, down dip from the Champion Delta. We focus on the shallow sedimentary section positioned between the seafloor and 0.4 s of two-way travel time (TWT) beneath the seafloor. The spectral amplitude roll-off for this portion of the seismic volume is near 80 Hz, providing a vertical resolution for deposit thickness on the order of 5 m. The entire survey was collected on a horizontal grid with $25 \text{ m} \times 25 \text{ m}$ spacing. The seismic reflectors defining the seafloor and two laterally persistent subsurface horizons were picked manually on every grid inline in order to produce the highest-quality set of maps for these three horizons. A digital elevation model (DEM) was created for each horizon by converting two-way time to depth. Depth conversion for the seafloor horizon assumed an average water-column velocity of 1500 m/s , and for the subsurface horizons we assumed an average velocity of 1700 m/s for the interval between the seafloor and the mapped horizon. This seismic velocity was measured for the first 300 m below seafloor, 60 km to the southwest of our study region (van Rensbergen et al., 1999).

OBSERVATIONS: SEAFLOOR MORPHOLOGY

The DEM of the continental shelf and slope offshore Brunei Darussalam shows several prominent morphological features (Fig. 2). The shelf edge lies at approximately 180 m water depth. On the upper continental slope there is a tributary network of channels extending $8 \text{ km} \times 24 \text{ km}$ in the strike and dip directions,

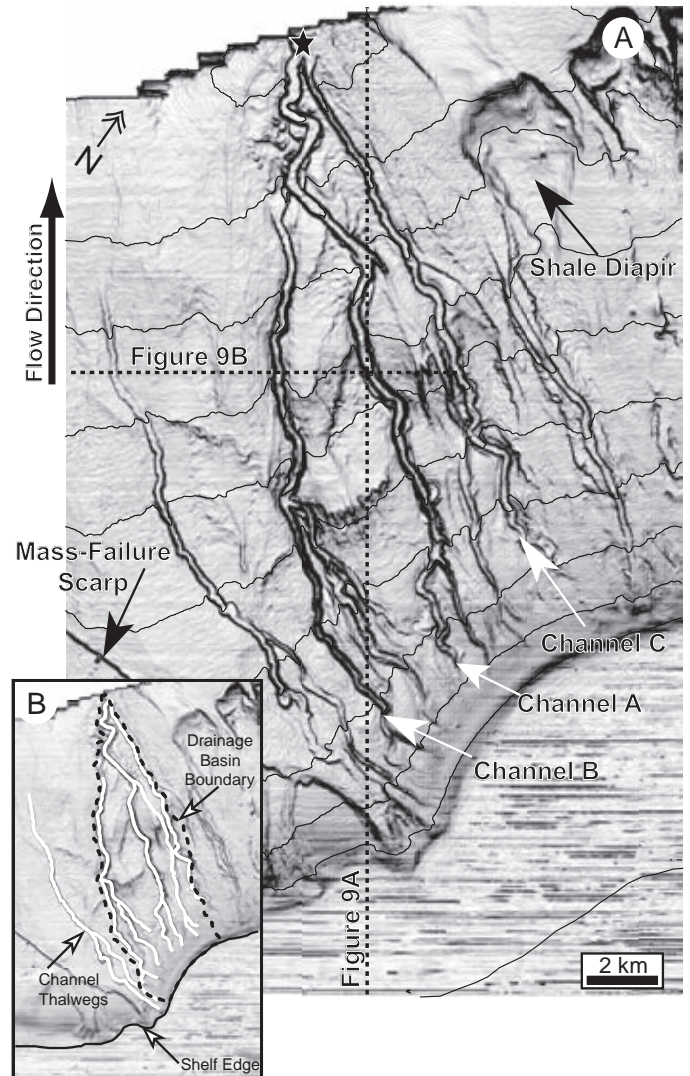


FIG. 2.—Maps of our study region in the South China Sea. **A)** Slope-magnitude map of study region highlighting the network of leaved submarine channels. This and other slope maps presented here were created by calculating the average absolute value for the local surface slope based on the surface elevations at each data bin and its eight immediate neighbors. High values of surface slope defining channel walls and detachment scarps have high gray-scale intensities (appear dark colored). Contour lines defining 100 m bathymetric intervals are superimposed on the dip map. Locations of seismic sections in Figure 9 are represented by dashed lines. Arrows and labels identify channels A, B, and C. Star denotes channel confluence referred to in Figure 3. **B)** Slope map with lines indicating interpreted location of shelf edge, 10 channel thalwegs, and margins of study drainage basin.

respectively. This network is positioned downslope of a large mass-failure scarp and within the topographic low produced following a mass-failure detachment. A prominent ridge is observed downslope of the tributary network of channels.

The average bathymetric profile of the continental slope in our study region is presented in Figure 3A, and its associated surface gradient is plotted in Figure 3B. This average profile is a

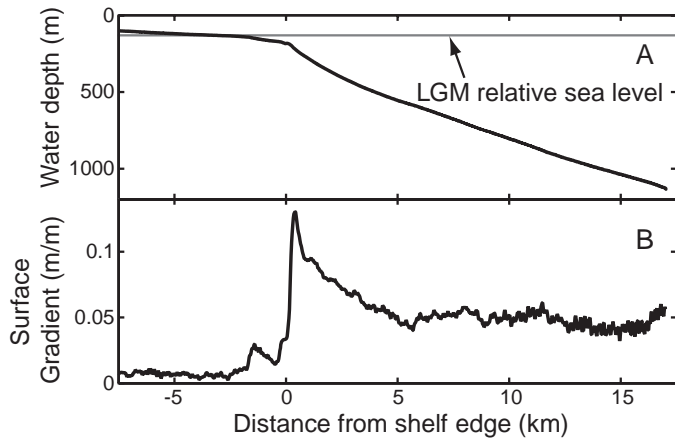


FIG. 3.—**A**) Bathymetry and **B**) downslope surface gradient swath profiles for the region of the Brunei continental shelf and slope offshore Champion delta. The location of LGM shoreline was calculated using model predictions from Milne and Mitrovica (2008) is noted in Part A.

swath profile calculated using water depth to the seafloor at every grid node in our study region as a function of distance from the shelf edge. This calculation takes advantage of the approximately 1,200,000 grid nodes in our study volume. The shelf edge was interpreted as the point of highest bathymetric curvature occurring in the transition zone between the overall low-gradient shelf (less than about 0.01) to the overall high-gradient slope (greater than about 0.05; Fig. 2B). With this boundary we calculated the shortest path length to the shelf edge for every grid node in our map of seafloor topography. Seafloor bathymetry was then sorted into bins of equal distance from the shelf edge, spaced every 25 m, and the average seafloor topography was then calculated for the points that fell into each bin. Downslope gradient was calculated at each node using the elevation difference between its upslope and downslope neighboring bins. The highest average surface gradients in our study area are positioned directly downslope from the shelf edge and are observed to be ~ 0.14 . This zone of high gradient is followed by a zone in which surface gradient decreases rapidly to a value of 0.05. Farther downslope, the surface gradient persists at the relatively constant value of 0.05 (Fig. 3B).

Analytical Techniques

The tributary channel network in our study area is composed of 10 channels that initiate 1–2 km downslope of the shelf edge. We extract long profiles for each of these 10 channels using our seafloor DEM in a manner analogous to the analysis of terrestrial drainage basin by Snyder et al. (2000). This process uses the accumulation of upstream drainage-basin area to define the locations of channels. In terrestrial settings, drainage-basin area associated with any one grid node is calculated by tracking all upstream grid nodes that have a steepest path of descent that feeds into the grid node in question. In the terrestrial environment, the upslope boundary of a drainage basin is associated with topographic highs that separate the path of fluid flow between neighboring basins. This definition must be modified for submarine drainage basins because they are linked to the shelf and terrestrial environments upslope. For this study we assume that submarine flow events initiate at the edge of the continental shelf and use this to define the upslope extent of drainage basins as

proposed by Straub et al. (2007). The lateral divides of our drainage basin downslope of the shelf edge are then defined in the same way as is done in terrestrial studies: that is, they are lines separating steepest paths of descent that result in flow paths terminating at the downslope confluence of our study basin (Fig. 2A) from flow paths that terminate in neighboring basins. The boundary of our study basin is presented in Figure 2B. The location for the head of each channel was defined by grid nodes that have an associated drainage-basin area in excess of 2 km^2 . This value of area ensures consistency between head locations selected by the DEM analysis and identified on the slope-magnitude map of seafloor topography. This method is similar to Montgomery and Dietrich's (1988) method for identifying terrestrial channel heads. In addition, this definition also corresponds to locations where channels reach a sufficient depth to be visible on our seafloor map. All 10 channels increase rapidly in relief from 0 m at a distance of $\sim 1\text{--}2$ km below the shelf edge to an average value of 40 m approximately 7 km downslope of the shelf edge. The three major trunk channels maintain this roughly constant relief for the remainder of their lengths. A plot of channel thalweg profiles is presented as Figure 4. In this figure, profiles are aligned with distance from the distal-most channel confluence in the network. Gradients for the low-order channels average ~ 0.07 , compared to an average gradient for the trunk channels of ~ 0.05 . Knickpoints occur at several of the channel confluences.

Channel relief was measured for 1921 channel cross sections within the study network. For 206 of these channel cross sections, channel width was also measured. This number of measurements of channel relief and width allowed us to assess the relationship between these two parameters. Cross sections were oriented approximately perpendicular to the direction of the local channel centerline. Channel width was defined as the horizontal distance between levee crests. Channel relief was measured as the elevation difference between the average water depth for the two levee crests and the channel thalweg. We used the seismic data to determine if channel reliefs had been altered by deposition from post-abandonment sedimentation (largely resulting from overbanking flow of neighboring channels). Channels that had been altered by post-abandonment deposition were then excluded from our analysis. A cross-plot of channel width and relief is presented in Figure 5. We observe a linear increase in channel width with increases in channel relief. The observed trend suggests that for this particular system the channels have a minimum

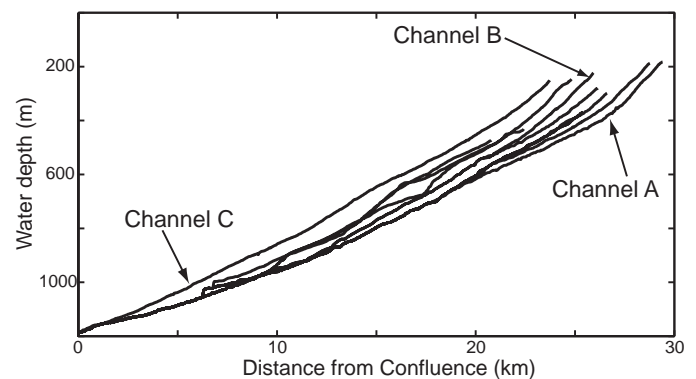


FIG. 4.—Long profiles of the ten submarine channels that comprise the tributary channel network on the continental slope of the Champion delta. Channel profiles are measured against distance from most distal confluence in network (Star in Figure 2B).

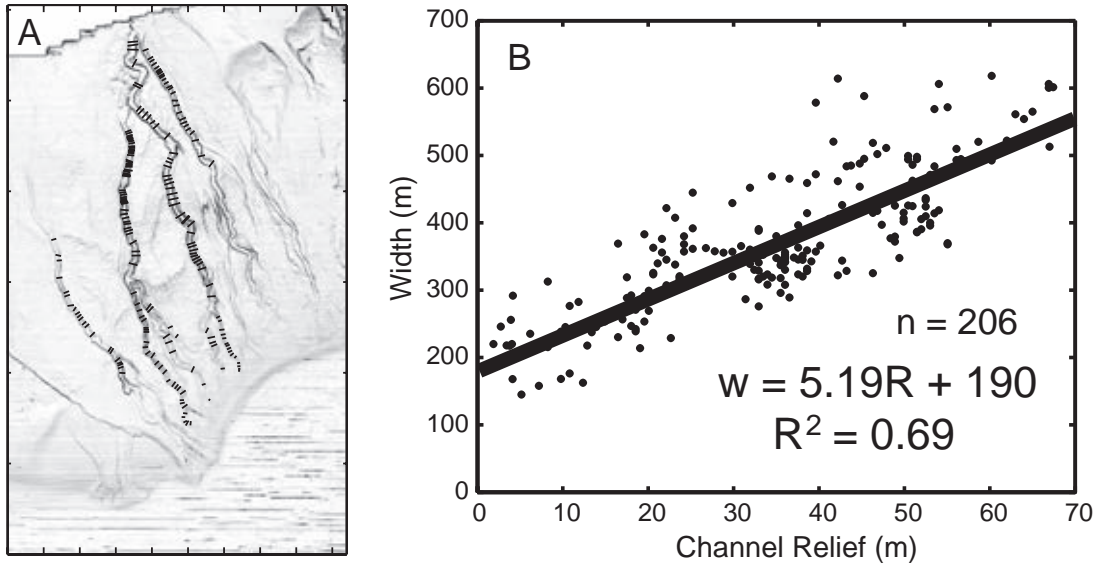


FIG. 5.—Channel width as a function of channel relief measured along 206 channel cross sections. **A)** Slope map with location of 206 channel cross sections used for width–relief comparison identified. **B)** Cross plot of channel width as a function of channel relief. The best-fit regression line of 206 measurements is shown by the solid black line.

width of approximately 200 m at the point of channel initiation (i.e., the channel head).

One of the goals of our study was to quantify correlations between channel dimensions and basin characteristics, including distance from the shelf edge and contributing drainage-basin area. The first set of parameters that we explore is the relationship between channel dimensions (width and relief) and distance from the shelf edge. To quantify these trends we calculated the shortest path length to the shelf edge for the midpoint of every measured channel cross section. The line describing the shelf edge is the same line used in calculating the swath profile (Fig. 2B). Channel width and relief were then sorted into bins of equal distance from the shelf edge (Fig. 6). Both mean channel width and relief increase rapidly between 4 and 8 km from the shelf edge, but then remain approximately constant with further distance from the shelf–slope break.

Next we assess how channel width and relief scale with upslope drainage-basin area. In terrestrial environments, several studies have observed power-law relationships between channel width and relief and upslope contributing drainage-basin area. In these studies the exponent, α , in the equation relating channel width to basin area,

$$w = A^\alpha \quad (1)$$

where A is drainage basin area and w is channel width, ranges between 0.4 and 0.55 (Church and Rood, 1983; Leopold, 1994; Leopold and Maddock, 1953). In the equation

$$R = A^\beta \quad (2)$$

relating channel relief (R), to A , the scaling exponent (β) ranges between 0.30 and 0.4 for terrestrial systems (Church and Rood, 1983; Leopold, 1994; Leopold and Maddock, 1953). We find that α ranges between 0.1 and 0.2 (Fig. 7A) and β ranges from 0.15 to 0.25 (Fig. 7B) for these two channels.

Next, to address surface morphological characteristics at channel heads we measured the long profiles of the three largest

channels in our network. To complement the swath-profile data presented in Figure 3, we also measured the channel gradient along these three long profiles (Fig. 8). For each channel long profile the location of the channel head is estimated using the grid node on a channel long profile that has an associated drainage-basin area in excess of 2 km². We also extend these channel profiles upslope of the channel head by tracking the path of steepest ascent. For these three profiles the channel heads are

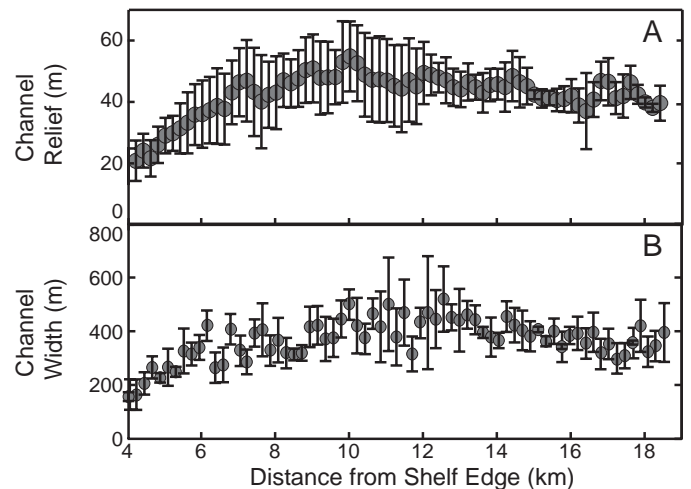


FIG. 6.—Plots defining the change in mean channel-morphology parameters as a function of distance from the shelf edge. Error bars on all plots correspond to \pm one standard deviation of data in each bin. **A)** Mean channel relief sorted in bins as a function of distance from the shelf edge (bin width of 250 m). Channel-relief trend is computed from 1921 channel cross sections. **B)** Mean channel width as a function of distance from the shelf edge (bin width of 250 m). Channel-width trend computed from 206 channel cross sections.

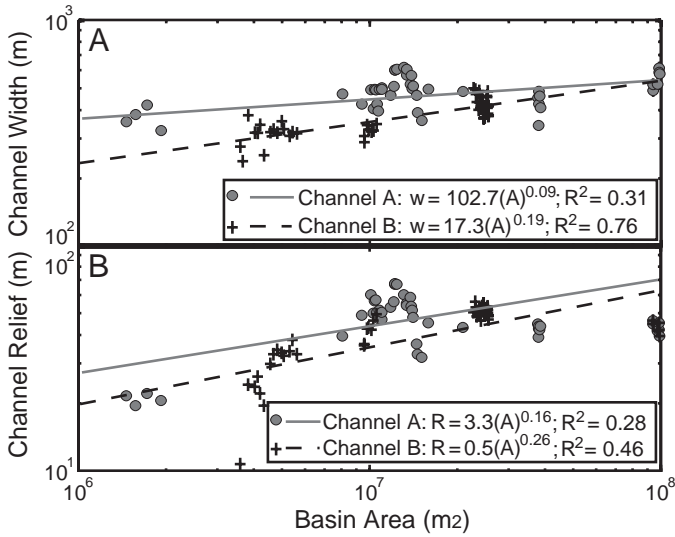


FIG. 7.—Plots defining change in channel morphology parameters (width and relief) as a function of upslope contributing drainage-basin area for channels A and B. **A)** Channel width as a function of drainage-basin-area. **B)** Channel relief as a function of drainage-basin-area.

located between 1 km and 2 km downslope of the location of maximum gradient along the profiles. Additionally, the location of maximum channel gradient for these three systems exists between the shelf-slope break and the channel heads.

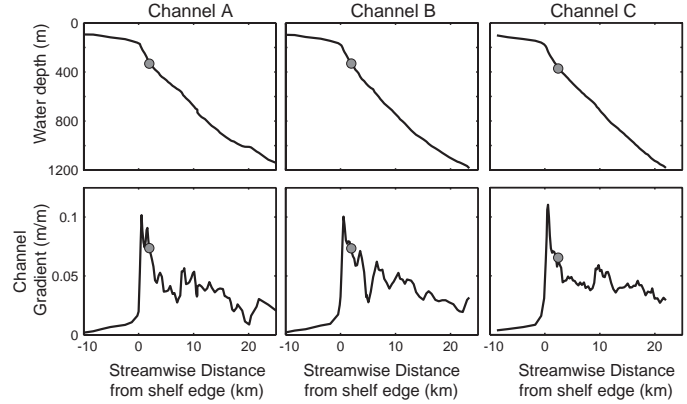


FIG. 8.—Long profiles of bathymetry and down-channel surface gradient for channels A–C with locations of the channel heads marked on each plot by a gray circle (the point at which channels begin to be resolved on topographic map with 5 m vertical resolution). Upslope of the channel head, the long profile represents the steepest path of ascent (or descent).

OBSERVATIONS: SHALLOW SUBSURFACE ARCHITECTURE

Our study focuses on the section of stratigraphy preserved between the seafloor and a depth below seafloor defined acoustically at 0.4 s TWTT. To unravel the recent margin evolution we mapped two shallow regional surfaces (CD1 and CD2) (Fig. 9).

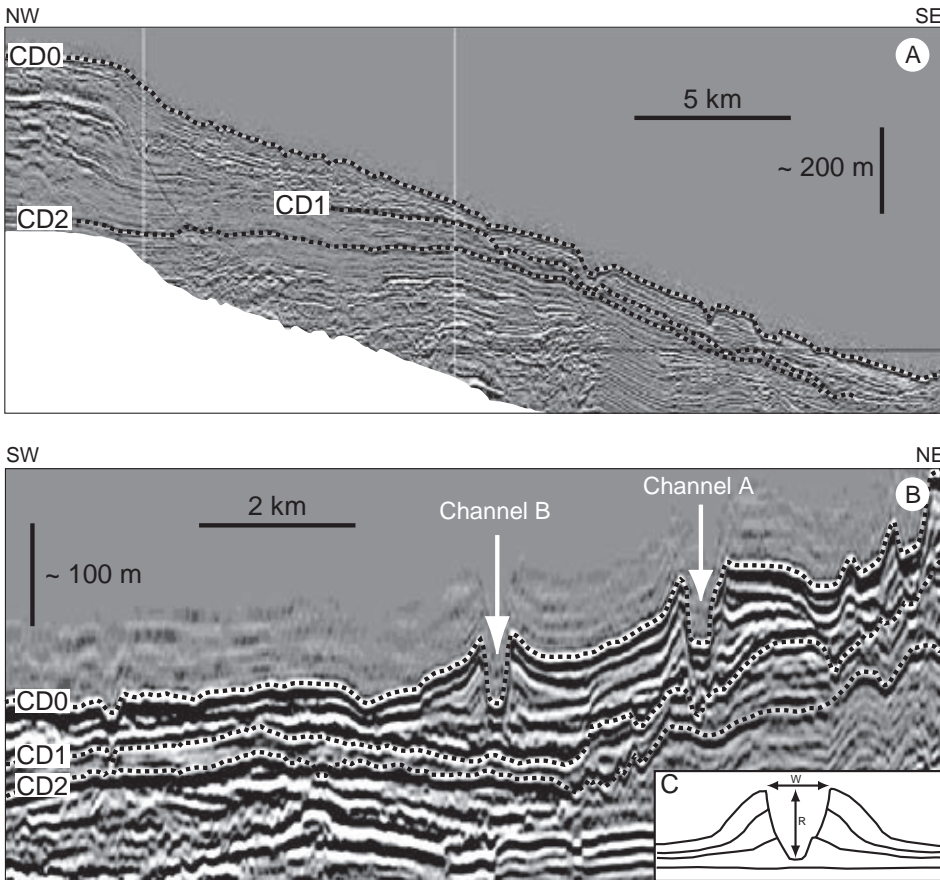


FIG. 9.—Characteristic dip- and strike-oriented seismic lines for the study region, showing a portion of the regional stratigraphy from the seafloor to below the area of interest in this study. The dashed lines labeled CD0–CD2 follow surface and subsurface horizons that represent the present-day seafloor and approximate paleo-seafloor locations. Locations of seismic cross sections are labeled in Figure 2. **A)** Characteristic dip section spanning the upper continental slope from the present-day continental shelf to 1200 m of water depth. **B)** Characteristic strike section. The section intersects channels A and B at close to right angles to the channel centerline. Seismic velocity increases with depth, so vertical scale is an approximate vertical average for the section. **C)** Definition sketch illustrating channel relief (R) and channel width (W).

These seismic horizons were selected because they have strong reflection amplitudes that can be traced regionally and are cross-cut only by local erosion in small patches. These characteristics allow us to track the surfaces beneath the majority of the area encompassed by the 10 channels in the study region (Fig. 10). Maps of these seismic horizons represent approximate paleobathymetry since there has been little deformation since accumulation of this interval. The lateral extents of surfaces CD1 and CD2 represent planform boundaries where outside of these boundaries we could no longer confidently map the stratigraphic location of the surface. At these boundaries strong-reflection-amplitude seismic horizons either transitioned to weak-reflection-amplitude horizons or to chaotic horizons. Biostratigraphic dates obtained from exploration wells located 60 km to the southwest of the study region suggest that both horizons are of Quaternary age (Hiscott, 2001). Both maps lack significant local topography associated with paleochannels, but they have features interpreted as failure scarps. On surface CD2 there is a failure scarp with 70–90 m of relief that is oriented roughly north–south (Fig.

10A). On surface CD1 a failure scarp is observed with 30–50 m of relief and a significant degree of variability in planform orientation (Fig. 10B). Downslope of the failure scarp on surface CD1, several long linear striations exist which might represent gouge marks formed during the release of a mass-failure event. The expression of this failure scarp and material removed during this failure is also seen on an isopach map measured between surfaces CD2 and CD1 (Fig. 11A). Deposits of material released during these mass failures are not found within the area covered by this seismic volume. The region of the continental slope affected by the two mapped mass-failure scarps exceeds 40 km² in each event.

Following the mass-failure release associated with the scarp on surface CD1, the continental slope downdip of the Champion delta has been a site of net deposition. A CD1-to-seafloor isopach map shows development of leveed channels on top of the regionally extensive and relatively smooth slide plane and provides us with the simplest possible initial condition for studying the evolution of aggradational submarine channels (Fig. 11B). Sev-

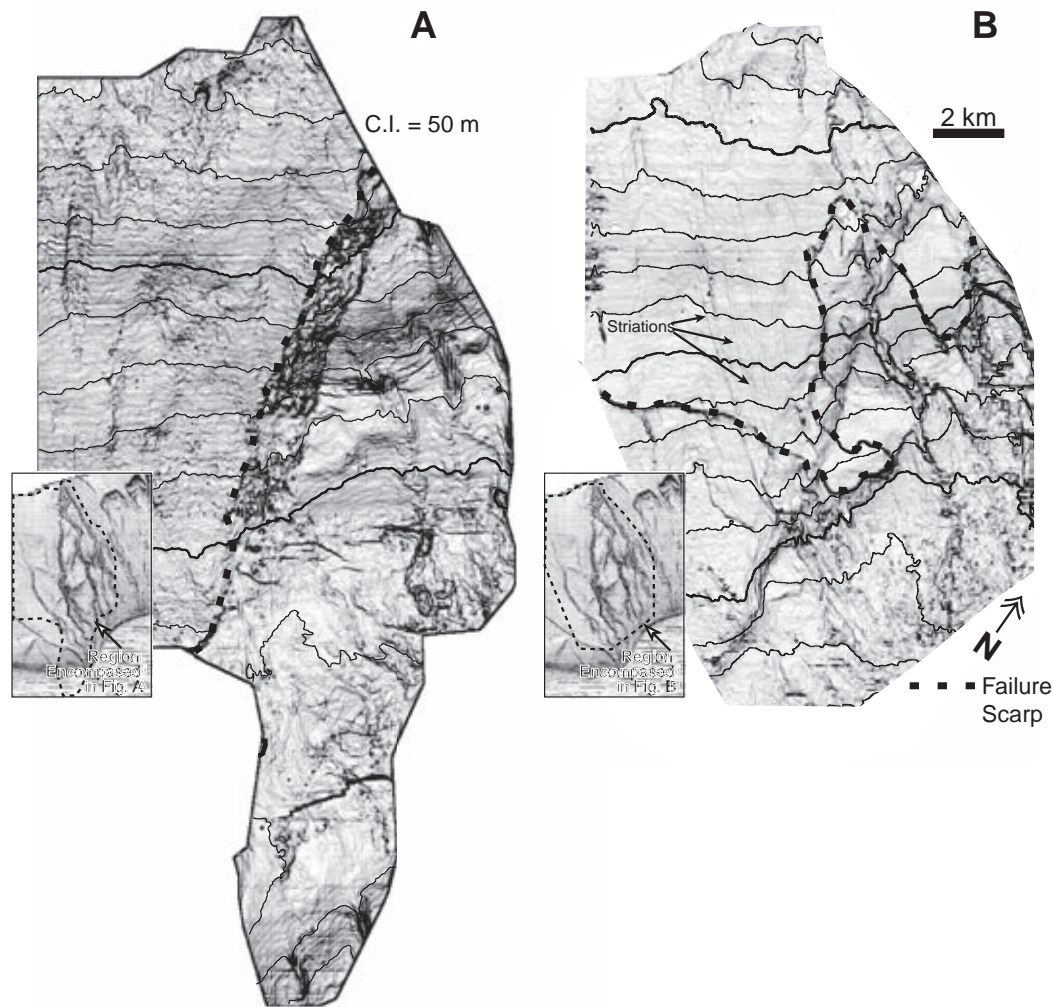


FIG. 10.—Maps of subsurface seismic horizons A) CD2 and B) CD1. Dashed lines mark the locations of failure scarps. The insert delineates the boundaries of the two maps. A) Slope map of regional subsurface horizon CD2. The horizon defines the scarp and slide plane associated with release of the mass failure. Contours define depth below the present-day seafloor. The contour interval is 50 m. B) Slope map of regional subsurface horizon CD1. The horizon defines the scarp and slide plane associated with the release of mass failure. Contours define depth below the present-day sea level.

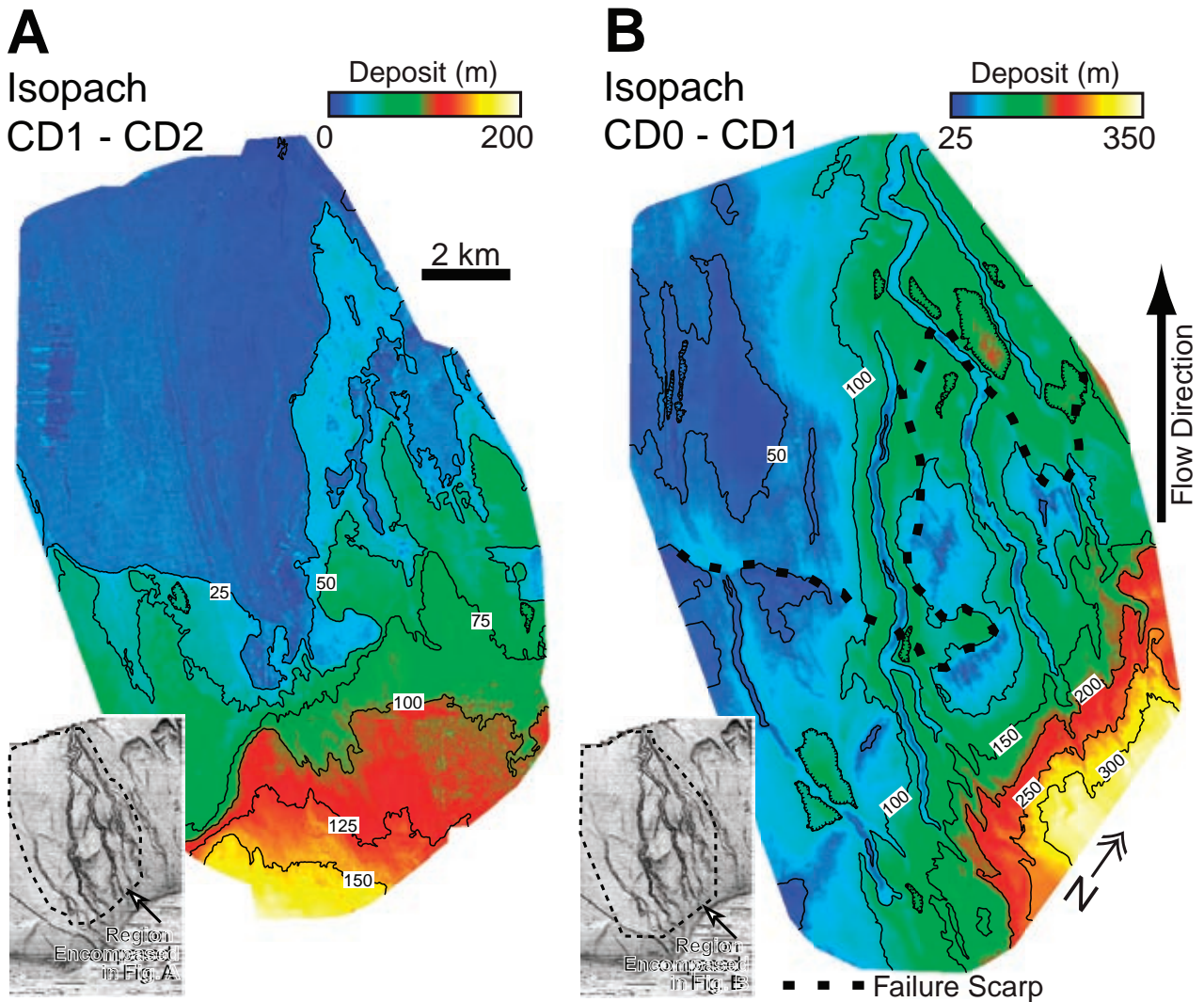


FIG. 11.—Maps of deposit thickness. **A)** Isopach measured between subsurface horizons CD1 and CD2. The contour interval is 25 m. The insert delineates the boundary of the map with respect to the study area. **B)** Isopach measured between the present-day seafloor (CD0) and subsurface horizon CD1. The contour interval is 50 m. The dashed line marks the location of the failure scarp. The insert delineates the boundary of the map with respect to the study area.

eral observations were made using the map of sediment thickness between surfaces CD1 and the seafloor ($\Delta\eta_{CD1-SF}$). There is a strong inverse relationship between distance from the shelf edge and deposit thickness. This observation supports work by Saller and Blake (2003) that this region of the Borneo margin is currently undergoing progradation. Deposition appears to be influenced by locally high surface gradients, associated with the subsurface mass-failure scarps (Fig. 12). Relative local lows in deposit thickness are present upslope of the scarp, and local deposit thickness highs are present downslope of the scarp.

Analytical Techniques

Deposition on an initially nonchannelized surface allow for the quantification of correlations between channel deposit thickness, channel gradient, channel relief, and distance from the shelf edge. A sequence of seismic lines oriented roughly perpendicular to the average downslope direction reveals that channel width and relief increase with downstream distance while deposit

thickness measured between the present-day seafloor and surface CD1 tends to decrease with distance from the shelf edge (Fig. 13). In order to evaluate the interdependence between these parameters we plot long profiles of channel relief and deposit thickness for channels A–C (Fig. 14). Deposit thickness is measured between the present-day elevation of a channel thalweg and that same location on map CD1. All three channel profiles show a rapid increase of channel relief between 0 to 5–7 km from their respective channel heads. This rapid increase is spatially correlated with a rapid decrease of in-channel deposit thickness for all three channels. Downslope of the initial increases in relief, all three channels reach an approximately constant channel relief for the remainder of the downslope region encompassed in our study area.

The observations defining correlations between channel relief and deposit thickness observed in Figure 14 aids interpretations of channelized depositional processes on the Brunei Darussalam margin. However, these observations use only a subset of the data defining depositional patterns on this margin. Our goal is to

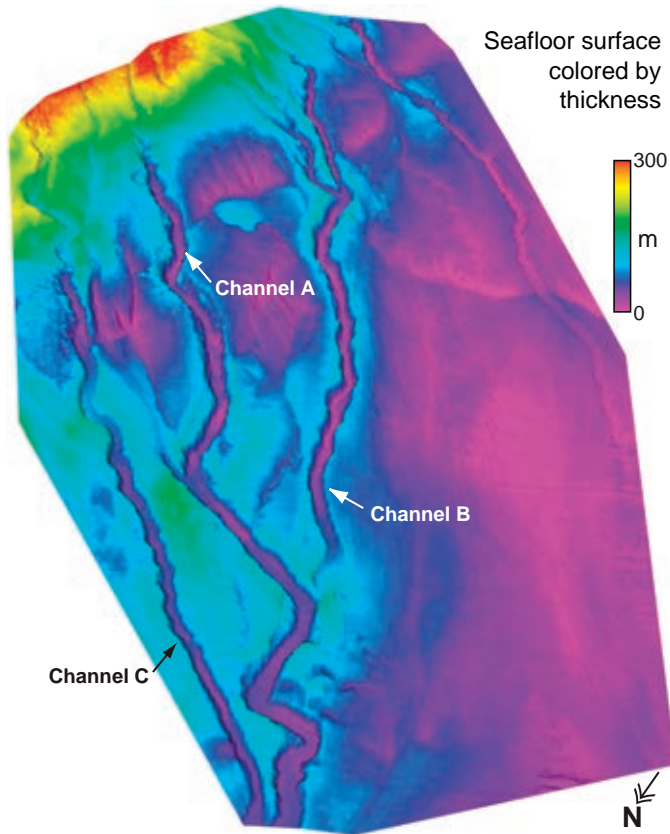


FIG. 12.—Three-dimensional view of the study region and submarine tributary network, colored with thickness of deposit between the present-day seafloor and subsurface horizon CD1.

characterize the depositional patterns resulting from channelized and unconfined, because both are responsible for the progradation of the slope. To accomplish this we analyze how deposit thickness, measured at every grid node in the thickness map, varies as a function of three properties: distance from the shelf edge, gradient of horizon CD1, and distance from a channel thalweg. These trends are described below.

To characterize how deposit thickness of $\Delta\eta_{\text{CD1-SF}}$ varies as a function of distance from the shelf edge we use the location of the shelf edge presented in Figure 2B. We calculate the shortest path length to the shelf edge for every grid node (in excess of 400,000 data points) in the thickness map, of $\Delta\eta_{\text{CD1-SF}}$, from which we can then relate thickness to distance from the shelf edge. We then binned the thickness data according to distance from the shelf edge using a bin size of 250 m. Mean deposit thickness and associated error bars as a function of distance from the shelf edge are shown in Figure 15A. The coefficient of variation (CV) associated with this data is presented in Figure 15B. CV is defined as the ratio of standard deviation of deposit thickness to mean deposit thickness in one data bin. We note a decay in deposit thickness with distance from shelf edge that is similar to that seen in the channel profiles of deposit thickness in Figure 14.

Next we characterize the importance of surface gradient on $\Delta\eta_{\text{CD1-SF}}$. We do this by comparing the maximum surface gradient for every grid node of the map defining the topography of surface CD1 with the deposit thickness associated with that grid node on

the map of $\Delta\eta_{\text{CD1-SF}}$. Maximum surface gradient for each grid node of horizon CD1 is defined as the maximum absolute surface gradient between a grid node and its eight neighboring nodes. We then sort data on deposit thickness into bins based on maximum surface gradient (Fig. 15C). No recognizable trend is observed between maximum surface gradient of the margin and resulting deposit thickness that exceeds the natural variability in the map.

The map of recent deposit thickness throughout the submarine-channel network contains the spatial information that defines levee form and magnitude of sediment accumulation on the distal overbank surface. Levee deposits are expected to gradually thin away from the channels (e.g., Figs. 9B, 11B). To characterize this depositional pattern we performed the following analysis. First, we identified the location of every grid node on the thickness map that corresponds to a thalweg of one of the 10 channels in the network (Fig. 2B). Using this network we calculated the path length to the nearest channel thalweg for every grid node. This allows us to examine every local measure of thickness as a function of distance from the closest channel thalweg. We then sort and assemble all of the data points according to distance from the closest channel with 25 m bins. Collapsing the data onto a single trendline allows us to capture both the mean depositional signal and the magnitude of variability about this trend associated with local topographic effects (Figs. 15D, 15E). It is worth noting that this method of analysis assumes that deposition at any node is associated only with the channel closest to this node, which might not be the case if channels are not contemporaneous. Utilizing this method, the results show that mean thickness thickens rapidly away from the thalweg until a maximum value near the levee crest, and then thins gradually until about 2 km from the thalweg. Beyond 2 km from the thalweg, the mean deposit thickness remains approximately constant at approximately 50 m.

DISCUSSION

What conditions are necessary for the initiation and construction of aggradational channel networks? An improved understanding of net aggradational networks is necessary for the modeling of continental-margin stratigraphy because they are the systems associated with transferring sediment to the subsurface. Our observations of recent erosional and depositional patterns on the continental slope offshore Brunei Darussalam indicate that the margin has experienced several large mass-wasting events during the Quaternary that appear to “clear” the slope and “reset” the topography. Following these large erosional events, however, turbidity currents have constructed intricate tributary channel networks through net deposition. The sediment accumulated on the upper slope in these channel networks represents the source of material for the mass failures. We have shown that these networks can arise with a slope aggradation of only 100 m.

While the construction of net aggradational submarine channel networks has not received significant attention from field-scale studies, the development of these systems has been studied in the laboratory. Yu et al. (2006) produced self-channelized subaqueous fans in an experimental basin. These experimental channelized fans were produced through the continuous feed of sediment-laden flow into an experimental basin. Unlike our study basin, the channel networks constructed and analyzed in the work by Yu et al. were distributary. Two critical conditions proposed for channel formation in that study were that input turbidity currents were unable to cover the entire area of the fan at any one time and that the currents contained relatively high amounts of clay-size material. The former condition resulted in

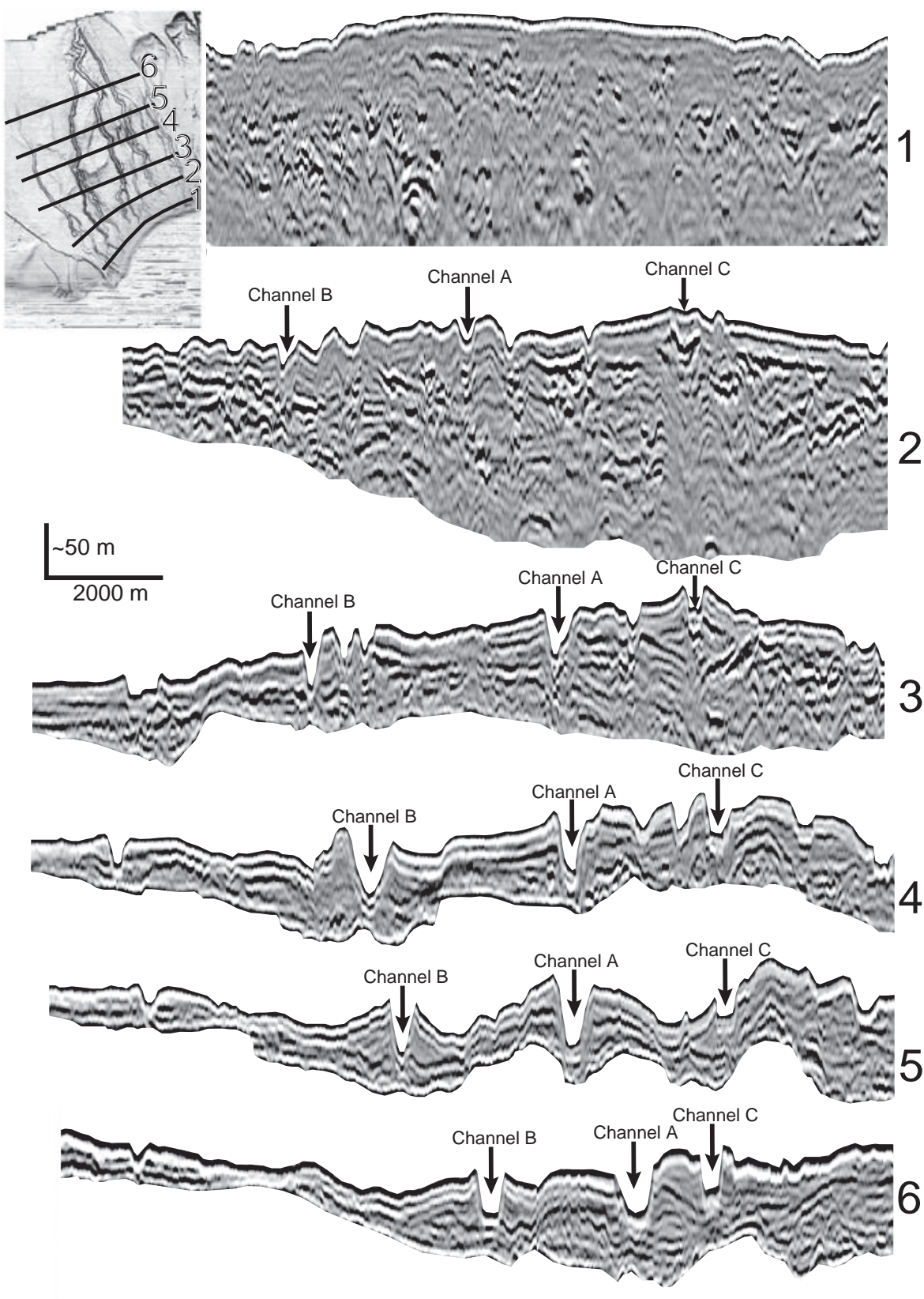


FIG. 13.—Seismic strike sections across the tributary channel network. For lines 2–6 seismic data between the seafloor and surface CD1 are shown. For line 1 seismic data are shown between the seafloor and a depth of 450 m below sea level.

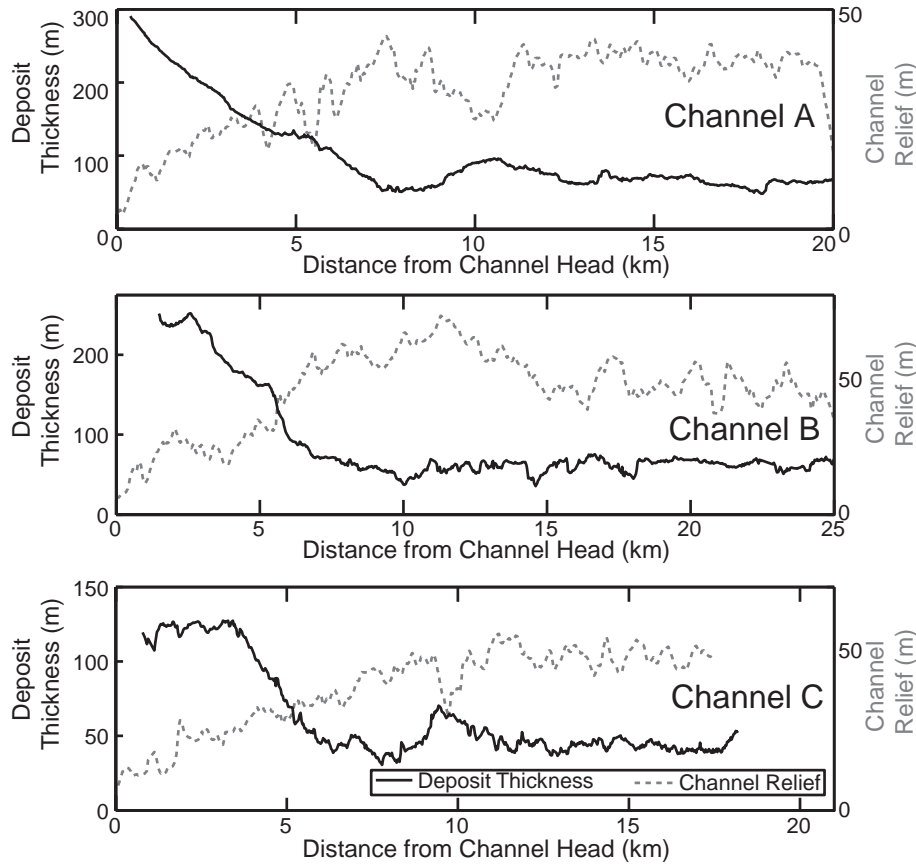


FIG. 14.—Downstream trends for thalwegs of Channels A, B, and C. For each downstream profile, channel relief and in-channel sediment thickness measured for the interval between the seafloor and subsurface horizon CD1 are plotted against distance from the channel head. The dashed line equals channel relief, and the solid line equals in-channel sediment thickness.

flow instabilities which aided channel formation. While input current widths were less than the basin width, they were also several orders of magnitude wider than the channels they formed, and several channels were active at any one time. In addition, current thickness was over an order of magnitude greater than the channels that the currents produced. These experimental conditions were associated with significant overbank sedimentation. Their visual observations also indicate that a rapid transition occurs in the steeper source area of the flow, from a nonchannelized area to an erosional area with channels. While we lack data defining channel-forming flow properties and our channel network is tributary in structure, the high overbank sedimentation rates in our study region suggest possible similarities between aggradational conditions in our field site and the experiments of Yu et al. (2006): namely that channel-forming flows were wider and thicker than the channels they formed and that multiple channels were likely active during any one flow. Below we utilize our observations to constrain conditions associated with channel initiation and flow properties.

Channel Initiation

Submarine channels on the continental slope offshore Brunei Darussalam do not connect to present-day fluvial channels. A broad continental shelf, 50–70 km wide, separates the present-day shoreline and the shelf edge. A number of seismic time slices through the shelf stratigraphy are shown in Figure 16. In these

time slices several features resembling meandering channels are visible in the shallow stratigraphy. However, none of these channel bodies are observed within 4–6 km of the shelf edge. Maps of paleo-shelf edges constructed from seismic and well-log data indicate that the modern shelf edge equates approximately to the shelf edge at the end of the Pleistocene (Saller and Blake, 2003; Sandal, 1996). Model predictions performed by Milne and Mitrovica (2008) place relative sea level during the last glacial maximum (LGM) at 120 ± 10 m less than the present-day sea level in our study region. Coupling the model predictions of Milne and Mitrovica and the paleo-shelf-edge maps of Saller and Blake, a 3–4 km separation between the shelf edge and the shoreline is predicted during the last glacial maximum for our study region (Fig. 3). This suggests that even during the LGM, a time of significantly low global sea level, a direct channelized link between submarine and terrestrial channels did not exist.

Several attributes of the present-day submarine channel network also suggest that most sediment transferred to the deep ocean did not occur through continuous fluvial to submarine channels. For example, average channel relief increases slowly from depths below the resolution of the seismic data (~ 5 m) 2 km downslope of the shelf edge to a stable depth of approximately 50 m at a distance of ~ 8 km downslope of the shelf edge, but channels are not observed on the seafloor over the first 2 km downslope of the shelf edge. Coupled to this is a linear increase in channel width with increases in channel depth (Fig. 6). Paleo-channel or canyon morphologies of resolvable scale are also not

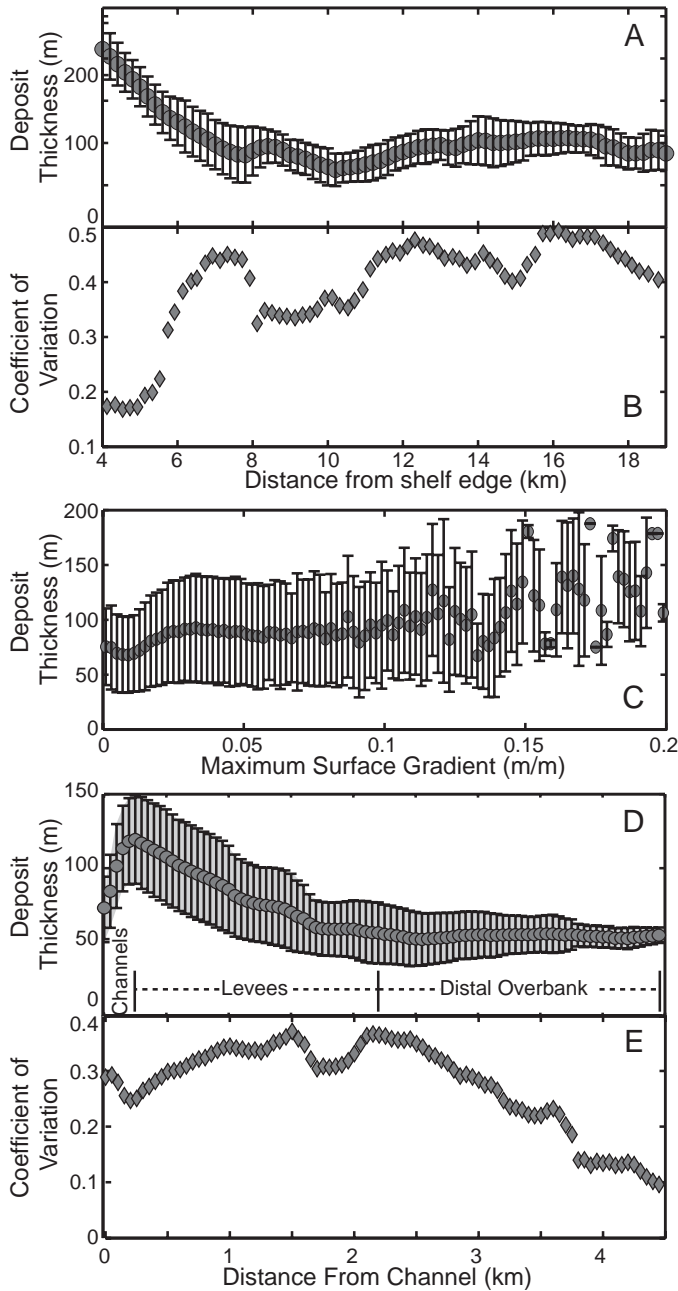


FIG. 15.—Plots defining change in mean deposit thickness as a function of three parameters: distance from the shelf edge, gradient of depositional surface, and distance from a channel thalweg in addition to mean channel relief as a function of distance from the shelf edge. Error bars on all plots correspond to \pm one standard deviation of data in each bin. **A)** Mean deposit thickness measured in bins spaced 25 m from the shelf edge. **B)** Mean channel relief measured in bins spaced 200 m from the shelf edge. Channel-relief trend is computed from 1921 channel cross sections. **C)** Mean deposit thickness measured in bins of 0.002 surface gradient of horizon CD1. **D)** Mean thickness of deposit measured in bins spaced every 25 m from closest channel thalweg. **E)** Coefficient of variation for deposit-thickness sample bins from Part D.

observed in seismic cross sections oriented perpendicular to the present-day submarine-channel network between the shelf edge and locations of channel heads (Fig. 13). While channel morphologies are not resolved in cross section, some threads of high seismic amplitude are observed between the seafloor and surface CD1 in the region encompassed in the first 2 km downslope of the shelf edge (Fig. 13, lines 1 and 2), particularly under channel C. These high-amplitude threads are possibly channelized sand deposits associated with channels linking the fluvial system to the deep-marine system. The width and thickness of these high-amplitude features and the lack of resolvable channel morphologies in seismic cross sections suggests that if continuous fluvial to submarine channels did exist they had depths less than 5–10 m over the first 2 km downslope of the shelf edge.

If direct channelized connections did not exist during the construction of the study channel network, how was sediment delivered to submarine-channel heads, and what processes resulted in the formation of the submarine-channel network? Previous studies of other continental-margin submarine channels have lacked direct links between terrestrial channels and submarine channels. Proposed mechanisms for sediment delivery to these submarine channels include large storms that evacuate sediment stored on broad continental shelves to the continental slope (Puig et al., 2003), cascading of cold, dense shelf waters (Canals et al., 2006), and breaching events along the shelf edge (van den Berg et al., 2002). Our observations and measurements of deposit thickness and channel relief as a function of distance from the shelf edge suggest that submarine channels in our study region formed as a result of sediment deposition from turbidity

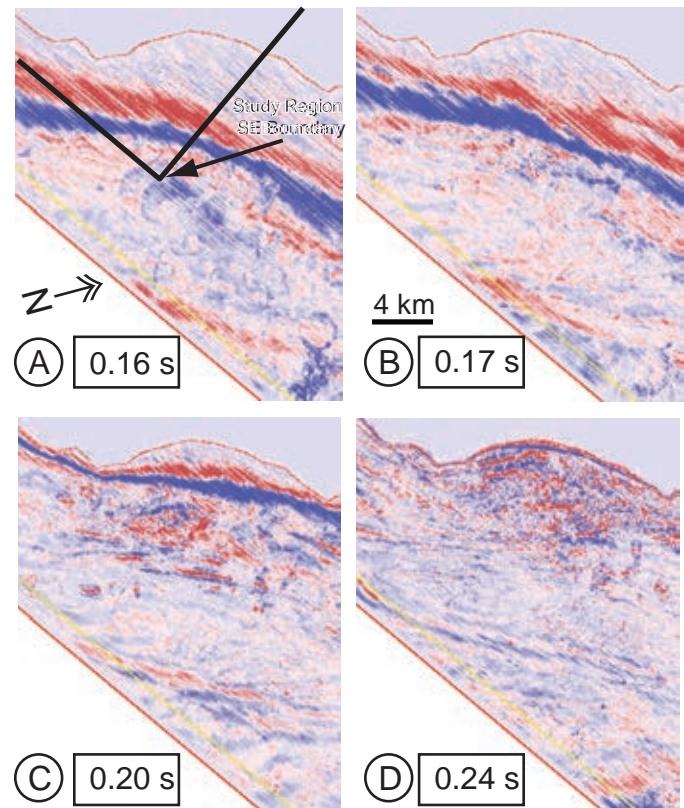


FIG. 16.—Time slices of the Champion Delta top at two-way travel times equal to **A)** 0.16 s, **B)** 0.17 s, **C)** 0.20 s, and **D)** 0.24 s. The location of the study region is outlined by the solid black line.

currents that initiated at the shelf edge, but the exact mechanism for initiation at this site is still unknown. All channels start at a similar distance, about 1 km downslope from the maximum downslope surface gradient, or about 2 km from the shelf edge (Fig. 8). This observation suggests a link between channel initiation and acceleration of currents over the shelf edge. Interesting recent studies by Izumi (2004) and Hall et al., (2008) found that flow thickness strongly influences channel spacing under net-erosional currents. A similar control on channel spacing might also exist in net-aggradational channels. The average channel spacing in the area near the shelf edge is approximately 1400 m. The recent theoretical work of Hall et al. (2008) indicates that submarine channels and gullies formed by sheet flows should have a spacing on the order of 25 times the thickness of turbidity currents. This would suggest a typical flow thickness of the order of 50 m for the channel-forming flows in our study region. Finally, measurements of channel width and relief are strongly correlated (Fig. 5). The best-fit trend suggests a width for channels at initiation (channel depth = 0) of 180 ± 50 m. This minimum width might be correlated to the scale of flow instabilities within sheet flows that are responsible for the initiation of channels. A control on channel width at channel initiation, similar to the control of channel spacing proposed by Izumi (2004) for currents initiating as sheet flows, might also exist and presents a future line of study.

If continuous fluvial to submarine channels did exist, but are unresolved in the first 2 km downslope of the shelf edge due to the seismic resolution of our data, it suggests that paleo-channels had reliefs less than ~ 10 m in this region. The depositional patterns on this margin also suggest that if continuous links did exist they were not effective at confining flows in the region just downslope of the shelf edge inasmuch as both channelized and unchannelized zones in this region have high deposition rates relative to the rest of the channel network.

Controls on Local Deposition

We use maps of recent deposition on the Brunei margin to quantify the correlation of three factors on deposit thickness: distance from the shelf edge, gradient of the depositional surface, and distance from a channel. The trends that we present in Figure 15 utilize data from both unconfined and channelized regions and thus allow us to access the importance of each factor as it relates to slope aggradation in the study area. As might be expected for net-depositional turbidity currents, we observe an initial decrease in mean deposit thickness with distance from the shelf edge. This decrease occurs between 4 and 8 km from the shelf edge, with a corresponding decrease in average deposit thickness from 225 m to 80 m. With additional distance from the shelf edge, mean deposit thickness remains approximately constant. Interestingly, we observe the opposite trend in mean channel relief with distance from the shelf edge. Between 4 to 8 km from the shelf edge the mean channel relief increases from 20 to 50 m and then remains approximately constant with further distance down slope. This trend is similar to the change in the coefficient of variation of deposit thickness as a function of distance from the shelf edge. To examine the correlation between mean channel relief and mean deposit thickness, we cross-plot these two parameters for data pairs that share the same distance from the shelf edge (Fig. 17). We note a strong anti-correlation between channel reliefs of 15 m to 55 m. We hypothesize that as currents construct deep channels the lateral confinement of turbidity currents increases. Presumably the spatial trends observed in the data also translate temporally. So, with time, levee aggradation increases channel relief and flow confinement. This lateral confinement focuses flow along pre-

ferred transport directions (i.e., following channel centerlines), which in turn increases the transport efficiency of currents.

Interestingly, we observe no trend in deposit thickness as a function of maximum surface gradient (Fig. 15C). Local regions of high slope associated with the failure scarp on surface CD1 have clearly affected depositional patterns on the margin (Figs. 11B, 12). However, in this study region the effect of surface gradient is not as strong as other factors (Fig. 15C).

The collapse of data on deposit thickness as a function of distance from a channel thalweg results in a trendline that is analogous to a mean channel–levee profile oriented perpendicular to a channel centerline. As such, this plot allows us to define and characterize three depositional zones within the network. The first zone makes up the channels themselves. Average channel half-width is 125 m, and over this distance deposit thickness increases from 72 m at the thalweg to 122 m at the levee crest (Fig. 15D). The second zone defines the average levee form and runs between 125 m to 2200 m from a channel centerline. Over this lateral distance, sediment thickness drops from 122 m at the levee crest to 55 m at its distal termination. It is not obvious where to place the distal end of the levee on the basis of mean thickness only. We refined the location by taking advantage of the spatial structure in the coefficient of variation for deposit thickness. Coefficient of variation maintains an approximately constant, relatively large value for a distance up to 2200 m from a channel center. After this point values for CV systematically decrease with increasing separation from a channel. We take the transition from a roughly constant CV to a continuously decreasing one as defining the boundary between the levee and the background overbank surface. We expect a greater variation in depositional thickness to be associated with focused levee deposition versus the background sedimentation building the regional overbank surface. Sedimentation on the distal overbank has produced a deposit with a nearly constant thickness of 55 m. With the length scales associated with each depositional zone defined, we have created a deposit facies map for our study region that delineates channel, levee, and distal overbank facies (Fig. 18).

Analysis of the three depositional zones reveals two system properties that are particularly relevant to inferring behavior of

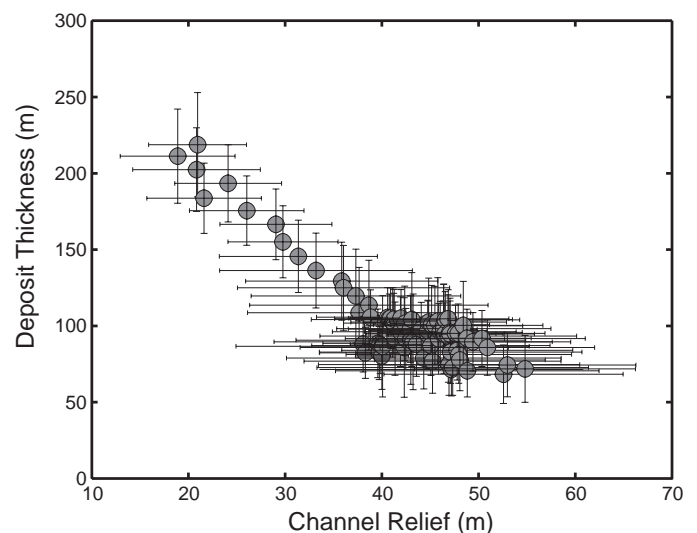


FIG. 17.—Cross plot of mean deposit thickness and mean channel relief for data binned as a function of distance from the shelf edge. Horizontal and vertical error bars represent \pm one standard deviation of data in each bin.

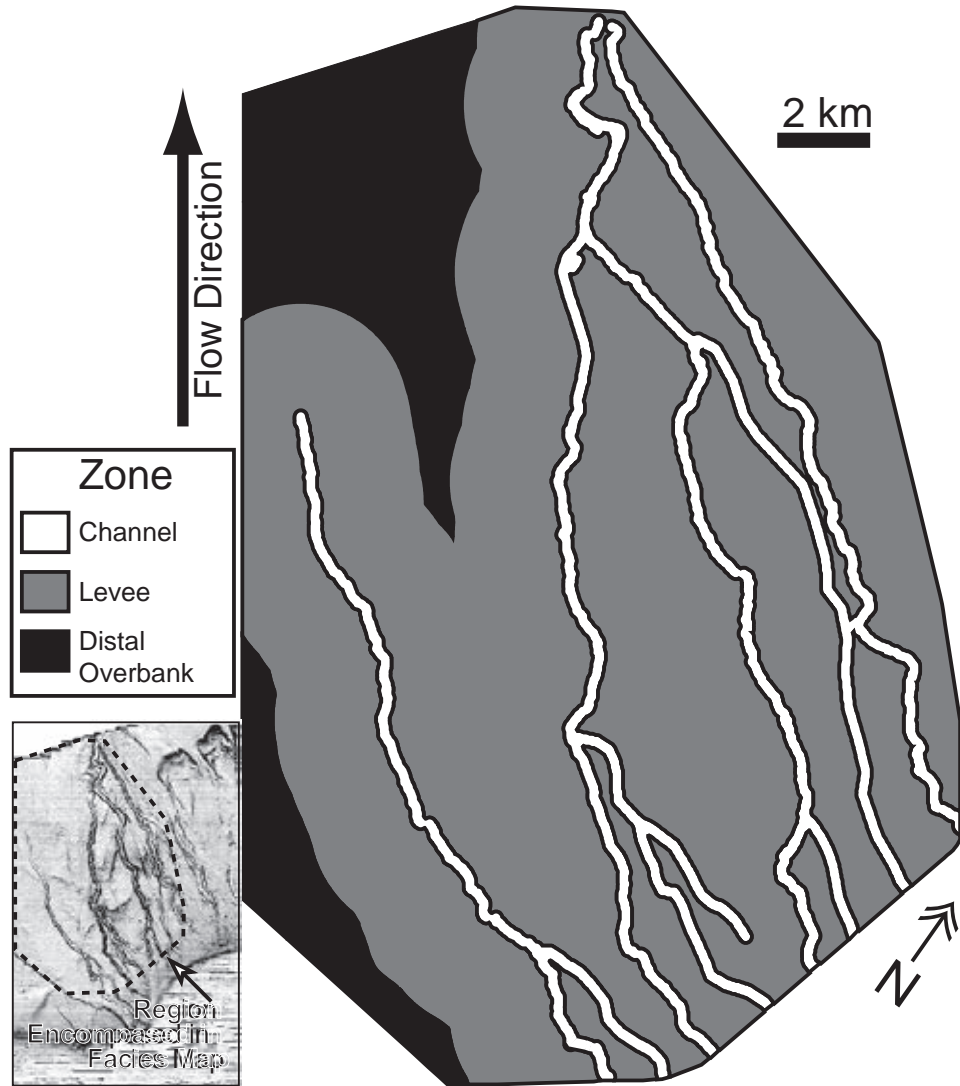


FIG. 18.—Facies map of three depositional zones in the Brunei Darussalam channel network: channel, levee, and distal overbank. Criteria used to define the zones is based on trends in deposit thickness measured as a function of distance from a channel thalweg as presented in Figures 14D and 14E.

the evolving network. First, sedimentation in channel thalwegs is only somewhat greater than the background deposition associated with the far-field overbank surface, 72 m versus 55 m (a ratio of 1.3), respectively. These nearly equal values of in-channel versus overbank deposit thickness point to development of channels that are laterally stable and thus are not rapidly becoming superelevated relative to their overbank surface. This slow development of superlevation suggests that the channels are not prone to frequent avulsion (Mohrig et al., 2000). Second, the characteristic half-width of the levee package is 8.4 times the average channel width ($w = 250$ m) (Fig. 15D). Because most channels in our study network are separated by less than 2 km from their closest neighboring channel (Fig. 18), this levee distance suggests that some fraction of overbanking flow from currents moving down one channel is likely to reenter an inactive or neighboring channel and continue to move downslope.

Our observations suggest that the two critical factors controlling deposit thickness in the study region are degree of current

confinement in channels flanked by prominent levees and distance from a channel thalweg. As the last step in this analysis we quantify the volume of sediment stored in the flow-confining levees relative to both the channel thalweg and the distal overbank. We accomplish this by first calculating the number of grid nodes located between 0 and 125 m (channel nodes), between 125 and 2200 m (levee nodes), and between 2200 and 4500 m (distal overbank nodes) from a channel thalweg. These values are then multiplied by the mean deposit thickness within each depositional zone. We find that 85% of the sediment recently deposited on the Brunei Darussalam margin is stored within channel levee nodes while 11% is stored in channel deposit nodes and 4% is stored in the distal overbank nodes (Table 1). In this network the approximate amount of sediment stored in levees is eight times greater than the amount of sediment stored in channel deposits.

Our findings indicate that construction of aggradational networks is largely tied to weakly channelized flows which are free to overbank into unconfined regions. In the most proximal area

TABLE 1.—Data defining area and volume of sediment contained within channel deposits, levee deposits, and distal overbank deposits.

| 17 km³ of slope deposit (area: 192 km²) | % of total area | % of total deposit volume |
|--|----------------------------|--------------------------------------|
| Channel bottom | 11 | 11 |
| Levee | 81 | 85 |
| Distal Overbank | 8 | 4 |

immediately below the shelf edge, flows are probably wide and too weak to develop channels. These flows may be plunging river plumes off the paleo-Champion delta, or the result of dense suspensions resulting from wave-induced stresses near the delta front or upper slope. As they accelerate downslope, flows begin to focus at sites where net deposition is less than in adjacent areas, forming aggradational channels. These flows then construct levees, which eventually become high enough to partially or completely confine flows within channels. As flows progressively become more confined through levee construction, local deposition rates decrease as sediment is funneled farther downstream before deposition can occur. This sedimentation pattern, which is associated with partially channelized flows, appears to be superimposed on a regional depositional pattern associated with hemipelagic sedimentation. The signal of the hemipelagic sedimentation is stored in the volume of sediment recorded in the distal overbank deposits.

Recent laboratory experiments reported by Mohrig and Buttlers (2007) document overbank deposition resulting from flows that were partially guided by a channel. In their experiments the ratio of mean channel-deposit thickness to mean overbank-deposit thickness was monitored for a series of flows that had different ratios of current thickness to channel relief. We found that the ratio of mean channel-deposit thickness to mean overbank-deposit thickness for the Brunei network was 1.3. This ratio corresponds to flows in excess of three times channel relief in the Mohrig and Buttlers (2007) experiments. Given a typical channel relief in our study region of 50 m, this suggests flow thicknesses on the order of 150 m. This value of flow thickness is significantly higher than the flow thickness estimated from the spacing of channel heads. We propose that the difference in these thickness estimates is partially related to the funneling of sheet flows into channels. The estimate of current thickness from the spacing of channel heads likely reflects the thickness of unconfined sheet flows. A thickening of turbidity currents is likely associated with the funneling of these sheet flows into channels as currents move downslope. This second estimate of flow thickness supports our assumption that the Brunei channel network was constructed by flows that were only partially confined, promoting high overbank deposition rates. It is also worth noting that the suggested thickening of flows in this tributary system is fundamentally different from the downslope evolution of flows in distributary networks (Normark et al., 1979; Pirmez and Flood, 1995; Yu et al., 2006), where channel relief and deposit thickness decreases with distance from the source of the current. The model of slope evolution for our study area is associated with deposition primarily in the form of levees (Fig. 19). As such, the construction of seascape evolution models for margins dominated by aggradational channels will require increased study into the fluid dynamics of overbanking turbidity currents and levee morphodynamics.

The proposed model for sediment delivery to the Brunei margin via sheet-flow turbidity currents is significantly different from the evolution of shelf-edge deltas and submarine channels

with continuous channel features extending from the terrestrial region into the deep ocean. For example, Sylvester et al. (this volume) used a high-resolution 3D seismic volume to study the seismic stratigraphy of the Pleistocene Fuji-Einstein system, which consists of a shelf-edge delta that is directly linked to and coeval with two submarine channel-levee systems. Unlike the network offshore Brunei, the Fuji-Einstein channels are single threaded and are not tributary in structure. In addition, unlike the net-aggradational Brunei channel system these submarine channels link to the shelf edge through erosional channel conduits. Interestingly, though, the development and evolution of the Fuji-Einstein system was associated with a significant amount of deposition in the overbank environment, which resulted in thick aggradational levee packages and sediment waves. It appears that even in systems with continuous terrestrial-submarine channels, turbidity currents are significantly thicker than the channels which guide them and thus result in high overbank deposition rates.

Comparing Terrestrial and Submarine Channel Networks

How does the morphology of this submarine tributary channel network compare to terrestrial tributary networks? We observed scaling exponents which relate channel relief and width to drainage-basin area that are significantly less than exponents describing terrestrial channel networks (Fig. 7). In terrestrial networks, the scaling of channel width and relief to drainage-basin area is often used as a proxy for how these variables scale as a function of water discharge (Howard, 1994; Whipple, 2004). The physical explanation for this correlation lies in the method of fluid input to terrestrial channel networks. If precipitation is independent of channel network pattern, it follows that rainfall capture increases more or less linearly with drainage-basin area. Overland and shallow subsurface flow follows local paths of steepest descent. As a result, contributing upslope area at any point in a channel network is a proxy for net fluid discharge. The observed scaling exponents of submarine channels in our study region indicate that channel width and relief increase more slowly for a given increase in drainage-basin area compared to terrestrial networks. In addition to the low value of the scaling exponents relative to terrestrial networks, the correlation coefficient of the scaling exponents is quite low. The weak coupling between channel dimensions and drainage-basin area in our study likely indicates that drainage-basin area is a poor proxy for flow discharge through submarine channels. This is likely due to the method of flow input to submarine systems. In the submarine environment discharge is determined primarily by network boundary conditions at the upslope perimeter of the drainage basin. While channel width and relief do not scale to drainage-basin area in a fashion similar to terrestrial networks, several authors have observed scaling exponents between channel length and channel slope as functions of drainage-basin area that are similar to terrestrial environments (Mitchell, 2005; Pratson and Ryan, 1996; Straub et al., 2007). Contrary to the findings in this work, Mitchell (2005) theorized that similar scaling exponents relating channel slope to basin area in submarine and terrestrial basins indicates that drainage-basin area can in fact be thought of as a proxy for flow discharge through submarine channels. We believe that our findings support the suggestion of Straub et al. (2007) that scaling exponents relating channel length and slope to drainage-basin area are the result of geometric inevitability and not to physical processes.

All terrestrial tributary channel networks are net erosional features over some portion of their drainage-basin area (Crosby and Whipple, 2006; Snyder et al., 2000; Willgoose et al., 1991).

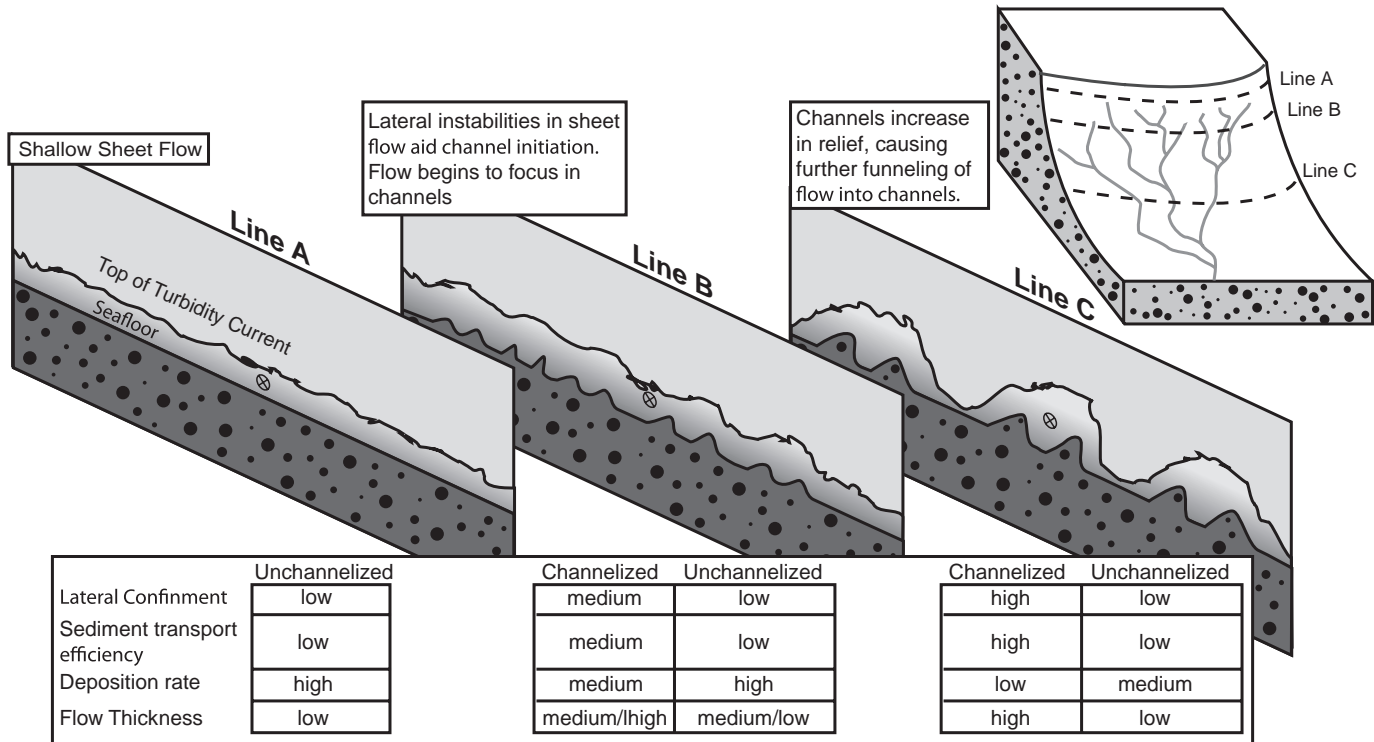


FIG. 19.—Conceptual model for processes responsible for channel formation and resulting flow–topography interactions on the Brunei Darussalam margin. Thin sheet flows initiate at the shelf edge and rapidly accelerate due to locally high surface gradients (Line A). Rapid acceleration of currents and flow instabilities results in spatially variable deposition rates and “proto-channels” (Line B). “Proto-channels” promote lateral confinement of flow along preferred transport directions, which aids construction of deep channels through levee deposition. This in turn increases the transport efficiency of a current and decreases deposition rates. This flow funneling also results in downslope thickening of currents (Line C).

Commonly, first-order channels are the most erosional portion of terrestrial tributary channel networks. Additionally, in most terrestrial networks a significant difference in channel slope exists between the first-order tributary channels and the network trunk channels. These differences in slope often exceed an order of magnitude where the low-order streams are often incisional and strongly coupled to their surrounding hillslopes (Willgoose et al., 1991). As such, these rivers strongly influence their local and regional gradient fields. Further, the strongly incisional nature of many terrestrial tributary systems does not allow flows to frequently overbank onto flood plains. All of the quantitative characteristics of the offshore Brunei tributary channel network that we have measured differ significantly from terrestrial networks. For example, the low-order tributaries of the Brunei network are only slightly steeper than their trunk channels (0.07 vs. 0.05). In addition, unlike terrestrial tributary networks, all parts of this network are net depositional, with the thickest deposits focused in and around the first-order channels. Unlike terrestrial channel systems, it is difficult to quantify the importance of channel-forming flow events to the gradient field of the Brunei margin. The current downslope gradient of the continental margin in our study region is similar to the downslope gradient of the slide planes imaged in the shallow subsurface (Fig. 10). Evidence from this and several other studies indicates that the Brunei margin frequently experiences mass-failure events that clear portions of the continental slope of channels (Demyttenaere et al., 2000; Gee et al., 2007). Clearly, the release of mass-failure events on this margin plays

a critical role in setting the slope gradient. However, conditions associated with the release of these mass-failure events might be influenced by the stratigraphy of deposits laid down during channelized flow events. Nonetheless it appears that identifying the influence of channelized flows on the gradient field of continental slopes is more difficult than in terrestrial environments.

CONCLUSIONS

Maps of the present-day seafloor and several subsurface stratigraphic horizons indicate that the Brunei continental margin experienced several large mass-wasting events followed by a change to net depositional conditions associated with the construction of a tributary submarine channel network. We used a map of deposit thickness associated with the construction of this network to quantify depositional trends of both the channelized and unconfined regions encompassed by this network.

The degree of turbidity-current confinement in deep channels and distance from a channel thalweg are the two strongest controls on slope deposition patterns. Trends describing mean deposit thickness and mean channel relief as functions of distance from the shelf edge are anti-correlated, indicating that current confinement in channels influences deposition rates. Data defining mean deposit thickness as a function of distance from a channel thalweg was used to quantify the volume of sediment associated with channels and levees in the network. We found that 85% of the sediment associated with this network resides in levees compared to 11% in channel deposits. These observations

suggest that this channel network offshore Brunei was largely constructed by flow events that were thicker than the channels they constructed and thus only marginally channelized. This style of channel evolution is fundamentally different from most terrestrial tributary channel networks, which are net erosional features.

ACKNOWLEDGMENTS

We thank Brunei Shell Petroleum and Abd-Rasak Damit for permission to publish seismic data from offshore Brunei Darussalam. Support for our research was provided by the STC Program of the National Science Foundation via the National Center for Earth-Surface Dynamics under agreement number EAR-0120914. Ben Sheets, Tommy Gerber, and Brad Prather are thanked for constructive reviews which greatly improved this manuscript. This study was initiated during a summer internship by the first author at Shell in Houston and was further developed as part of a Ph.D. dissertation at MIT. The Shell Turbidite Research Group provided valuable help and stimulating discussions in the early stages of this study.

REFERENCES

- ABREU, V., SULLIVAN, M., PIRMEZ, C., AND MOHRIG, D., 2003, Lateral accretion packages (LAPs): an important reservoir element in deep water sinuous channels: *Marine and Petroleum Geology*, v. 20, p. 631–648.
- BABONNEAU, N., SAVOYE, B., CREMER, M., AND KLEIN, B., 2002, Morphology and architecture of the present canyon and channel system of the Zaire deep-sea fan: *Marine and Petroleum Geology*, v. 19, p. 445–467.
- CAMPION, K.M., SPRAGUE, A.R., MOHRIG, D., LOVELL, R.W., DRZEWIECKI, P.A., SULLIVAN, M., ARDILL, J.A., JENSEN, G.N., AND SICKAFOOSE, D.K., 2000, Outcrop expression of confined channel complexes: Gulf Coast Section SEPM Foundation, 20th Annual Research Conference, Deep-Water Reservoirs of the World, p. 127–151.
- CANALS, M., PUIG, P., DE MADRON, X.D., HEUSSNER, S., PALANQUES, A., AND FABRES, J., 2006, Flushing submarine canyons: *Nature*, v. 444, p. 354–357.
- CANTERO, M.I., BALACHANDAR, S., AND GARCIA, M.H., 2007, High-resolution simulations of cylindrical density currents: *Journal of Fluid Mechanics*, v. 590, p. 437–469.
- CHURCH, M., AND ROOD, K., 1983, Catalogue of alluvial river data: Vancouver, B.C., Canada, Department of Geography, University of British Columbia, 103 p.
- CROSBY, B.T., AND WHIPPLE, K.X., 2006, Knickpoint initiation and distribution within fluvial networks: 236 waterfalls in the Waipaoa River, North Island, New Zealand: *Geomorphology*, v. 82, p. 16–38.
- DAMUTH, J.E., KOOLA, V.E., FLOOD, R.D., KAWSMANN, R.O., MONTEIRO, M.C., PALMA, J.J.C., AND BELDERSON, R.H., 1983, Distributary channel meandering and bifurcation patterns on Amazon Deep-Sea Fan as revealed by long-range side-scan sonar (GLORIA): *Geology*, v. 11, p. 94–98.
- DAS, H., IMRAN, J., PIRMEZ, C., AND MOHRIG, D., 2004, Numerical modeling of flow and bed evolution in meandering submarine channels: *Journal of Geophysical Research*, v. 109, p. 1–17.
- DEMYTTENAERE, R., TROMP, J.P., IBRAHIM, A., ALLMAN-WARD, P., AND MECKEL, T., 2000, Brunei deep water exploration: From sea floor images and shallow seismic analogues to depositional models in a slope-turbidite setting: Gulf Coast Section SEPM Foundation, 20th Annual Research Conference, Deep-Water Reservoirs of the World, p. 304–317.
- DENNIELOU, B., HUCHON, A., BEAUDOUIN, C., AND BERNÉ, S., 2006, Vertical grain-size variability within a turbidite levee: Autocyclicity or allocyclicity? A case study from the Rhone neofan, Gulf of Lions, Western Mediterranean: *Marine Geology*, v. 234, p. 191–213.
- DEPTUCK, M.E., STEFFENS, G.S., BARTON, M., AND PIRMEZ, C., 2003, Architecture and evolution of upper fan channel-belts on the Niger Delta slope and in the Arabian Sea: *Marine and Petroleum Geology*, v. 20, p. 649–676.
- GARCIA, M.H., AND PARKER, G., 1993, Experiments on the entrainment of sediment into suspension by a dense bottom current: *Journal of Geophysical Research*, v. 98, p. 4793–4807.
- GEE, M.J.R., UY, H.S., WARREN, J., MORLEY, C.K., AND LAMBIASE, J.J., 2007, The Brunei slide: A giant submarine landslide on the North West Borneo Margin revealed by 3D seismic data: *Marine Geology*, v. 246, p. 9–23.
- GERBER, T.P., AMBLAS, D., WOLINSKY, M.A., PRATSON, L.F., AND CANALS, M., 2009, A model for the long-profile shape of submarine canyons: *Journal of Geophysical Research*, v. 114, F03002, doi:10.1029/2008JF001190.
- GERBER, T.P., PRATSON, L.F., WOLINSKY, M.A., STEEL, R., MOHR, J., SWENSON, J.B., AND PAOLA, C., 2008, Cliniform progradation by turbidity currents: Modeling and experiments: *Journal of Sedimentary Research*, v. 78, p. 220–238.
- HALL, B., MEIBURG, E., AND KNELLER, B., 2008, Channel formation by turbidity currents: Navier-Stokes-based linear stability analysis: *Journal of Fluid Mechanics*, v. 615, p. 185–210.
- HISCOTT, R.N., 2001, Depositional sequences controlled by high rates of sediment supply, sea-level variations, and growth faulting: the Quaternary Baram Delta of northwestern Borneo: *Marine Geology*, v. 175, p. 67–102.
- HODGSON, D.M., FLINT, S.S., HODGETTS, D., DRINKWATER, N.J., JOHANNESSEN, E.P., AND LUTHI, S.M., 2006, Stratigraphic evolution of fine-grained submarine fan systems, Tanqua depocenter, Karoo Basin, South Africa: *Journal of Sedimentary Research*, v. 76, p. 20–40.
- HOWARD, A.D., 1994, A detachment-limited model of drainage basin evolution: *Water Resources Research*, v. 39, p. 2261–2285.
- HUANG, H., IMRAN, J., AND PIRMEZ, C., 2007, Numerical modeling of poorly sorted depositional turbidity currents: *Journal of Geophysical Research*, v. 112, C01014, doi 10.1029/2006JC003778/.
- IZUMI, N., 2004, The formation of submarine gullies by turbidity currents: *Journal of Geophysical Research*, v. 109, no. C03048, doi: 10.1029/2003JC001893.
- KOSTIC, S., PARKER, G., AND MARR, J.G., 2002, Role of turbidity currents in setting the foreset slope of cliniforms prograding into standing fresh water: *Journal of Sedimentary Research*, v. 72, p. 353–362.
- LEOPOLD, L.B., 1994, *A View of the River*: Cambridge, Massachusetts, Harvard University Press, 312 p.
- LEOPOLD, L.B., AND MADDOCK, T., 1953, The hydraulic geometry of stream channels and some physiographic implications: U.S. Geological Survey, Professional Paper 252, 56 p.
- MCGILVERY, T.A., AND COOK, D.L., 2003, The influence of local gradients on accommodation space and linked depositional elements across a stepped slope profile, offshore Brunei, in Roberts, H.H., ed., *Shelf Margin Deltas and Linked Down Slope Petroleum Systems: Global Significance and Future Exploration Potential*: Gulf Coast Section SEPM Foundation, p. 387–419.
- METIVIER, F., LAJEUNESSE, E., AND CACAS, M.C., 2005, Submarine canyons in the bathtub: *Journal of Sedimentary Research*, v. 75, p. 6–11.
- MILNE, G.A., AND MITROVICA, J.X., 2008, Searching for eustasy in deglacial sea-level histories: *Quaternary Science Reviews*, v. 27, p. 2292–2302.
- MITCHELL, N.C., 2005, Interpreting long-profiles of canyons in the USA Atlantic continental slope: *Marine Geology*, v. 214, p. 75–99.
- MITCHELL, N.C., 2006, Morphologies of knickpoints in submarine canyons: *Geological Society of America, Bulletin*, v. 118, p. 589–605.
- MOHRIG, D., AND BUTTLES, J., 2007, Shallow channels constructed by deep turbidity currents: *Geology*, v. 35, p. 155–158.
- MOHRIG, D., HELLER, P.L., PAOLA, C., AND LYONS, W.J., 2000, Interpreting avulsion process from ancient alluvial sequences: Guadalope-Matarranya (northern Spain) and Wasatch Formation (western Colorado): *Geological Society of America, Bulletin*, v. 112, p. 1787–1803.
- MONTGOMERY, D.R., AND DIETRICH, W.E., 1988, Where Do Channels Begin: *Nature*, v. 336, p. 232–234.

- MORLEY, C.K., 2007, Interaction between critical wedge geometry and sediment supply in a deep-water fold belt: *Geology*, v. 35, p. 139–142.
- NORMARK, W.R., PIPER, D.J.W., AND HESS, G.R., 1979, Distributary channels, sand lobes and mesotopography of Navy submarine fan, California Borderland, with applications to ancient fan sediments: *Sedimentology*, v. 26, p. 749–774.
- PEAKALL, J., AMOS, K.J., KEEVIL, G.M., BRADBURY, P.W., AND GUPTA, S., 2007, Flow processes and sedimentation in submarine channel bends: *Marine and Petroleum Geology*, v. 24, p. 470–486.
- PIRMEZ, C., AND FLOOD, R.D., 1995, Morphology and structure of Amazon channel, in Flood, R.D., Piper, D.J.W., Klaus, A., and Peterson, L.C., eds., *Proceedings of the Ocean Drilling Program, Initial Results*, v. 155: College Station, TX, Ocean Drilling Program, p. 23–45.
- PIRMEZ, C., AND IMRAN, J., 2003, Reconstruction of turbidity currents in Amazon Channel: *Marine and Petroleum Geology*, v. 20, p. 823–849.
- PIRMEZ, C., BEAUBOUF, R.T., FRIEDMANN, S.J., AND MOHRIG, D., 2000, Equilibrium profile and baselevel in submarine channels: examples from Late Pleistocene systems and implications for the architecture of deepwater reservoirs: *Gulf Coast Section SEPM Foundation, 20th Annual Research Conference, Deep-Water Reservoirs of the World*, p. 782–805.
- POSAMENTIER, H.W., AND KOLLA, V.E., 2003, Seismic geomorphology and stratigraphy of depositional elements in deep-water settings: *Journal of Sedimentary Research*, v. 73, p. 367–388.
- POSAMENTIER, H.W., AND WALKER, R.G., 2006, Deep-water turbidites and submarine fans, in Walker, R.G., and Posamentier, H.W., eds., *Facies Models Revisited: SEPM, Special Publication 84*, p. 397–520.
- PRATSON, L.F., AND RYAN, W.B.F., 1996, Automated drainage extraction in mapping the monterey submarine drainage system, California margin: *Marine Geophysical Researches*, v. 18, p. 757–777.
- PRATSON, L.F., NITTRouer, C.A., WIBERG, P.L., STECKLER, M.S., SWENSON, J.B., CACCHIONE, D.A., KARSON, J.A., MURRAY, A.B., WOLINSKY, M.A., GERBER, T.P., MULLENBACH, B.L., SPINNELLI, G.A., FULTHORPE, C.S., O'GRADY, D.B., PARKER, G., DRISCOLL, N.W., BURGER, R.L., PAOLA, C., ORANGE, D.L., FIELD, M.E., FRIEDRICH, C.T., AND FEDELE, J.J., 2007, Seascape evolution on clastic continental shelves and slopes, in Nittrouer, C.A., Austin, J.A., Field, M.E., Kravitz, J.H., Syvitski, J.P.M., and Wiberg, P.L., eds., *Continental Margin Sedimentation: From Sediment Transport to Sequence Stratigraphy*: Malden, Massachusetts, Blackwell, p. 339–380.
- PUIG, P., OGSTON, A.S., MULLENBACH, B.L., NITTRouer, C.A., AND STERNBERG, R.W., 2003, Shelf-to-canyon sediment-transport processes on the Eel continental margin (northern California): *Marine Geology*, v. 193, p. 129–149.
- PYLES, D.R., 2008, Multiscale stratigraphic analysis of a structurally confined submarine fan: Carboniferous Ross Sandstone, Ireland: *American Association of Petroleum Geologists, Bulletin*, v. 92, p. 557–587.
- SALLER, A., AND BLAKE, G., 2003, Sequence stratigraphy and syndepositional tectonics of upper Miocene and Pliocene deltaic sediments, offshore Brunei Darussalam, in Hasan Sidi, F., ed., *Tropical Deltas of Southeast Asia—Sedimentology, Stratigraphy, and Petroleum Geology: SEPM, Special Publication 76*, p. 219–234.
- SANDAL, S.T., 1996, The geology and hydrocarbon resources of Negara Brunei Darussalam: Brunei Darussalam, Brunei Shell Petroleum Company Sendirian Berhad and Brunei Museum, 243 p.
- SMITH, R., 2004, Silled sub-basins to connected tortuous corridors: sediment distribution systems on topographically complex sub-aqueous slopes, in Lomas, S.A., and Joseph, P., eds., *Confined Turbidite Systems: Geological Society of London, Special Publication 222*, p. 23–43.
- SNYDER, N.P., WHIPPLE, K.X., TUCKER, G.E., AND MERRITTS, D.J., 2000, Landscape response to tectonic forcing: Digital elevation model analysis of stream profiles in the Mendocino triple junction region, northern California: *Geological Society of America, Bulletin*, v. 112, p. 1250–1263.
- SPINNELLI, G.A., AND FIELD, M.E., 2001, Evolution of continental slope gullies on the northern California margin: *Journal of Sedimentary Research*, v. 71, p. 237–245.
- STEFFENS, G.S., BIEGERT, E.K., SUMNER, H.S., AND BIRD, D., 2003, Quantitative bathymetric analyses of selected deepwater siliciclastic margins: receiving basin configurations for deepwater fan systems: *Marine and Petroleum Geology*, v. 20, p. 547–561.
- STRAUB, K.M., AND MOHRIG, D., 2008, Quantifying the morphology and growth of levees in aggrading submarine channels: *Journal of Geophysical Research*, v. 113, Paper F03012, doi: 10.1029/2007JF000896.
- STRAUB, K.M., AND MOHRIG, D., 2009, Constructional canyons built by sheet-like turbidity currents: observations from offshore Brunei Darussalam: *Journal of Sedimentary Research*, v. 79, p. 24–39.
- STRAUB, K.M., JEROLMACK, D.J., MOHRIG, D., AND ROTHMAN, D.H., 2007, Channel network scaling laws in submarine basins: *Geophysical Research Letters*, v. 34, Paper L12613, doi: 10.1029/2007GL030089.
- STRAUB, K.M., MOHRIG, D., MCELROY, B., BUTTLES, J., AND PIRMEZ, C., 2008, Interactions between turbidity currents and topography in aggrading sinuous submarine channels: A laboratory study: *Geological Society of America, Bulletin*, v. 120, p. 368–385.
- VAN DEN BERG, J.H., VAN GELDER, A.V., AND MASTBERGEN, D.R., 2002, The importance of breaching as a mechanism of subaqueous slope failure in fine sand: *Sedimentology*, v. 49, p. 81–95.
- VAN RENSBERGEN, P., MORLEY, C.K., ANG, D.W., HOAN, T.Q., AND LAM, N.T., 1999, Structural evolution of shale diapirs from reactive rise to mud volcanism: 3D seismic data from the Baram delta, offshore Brunei, Darussalam: *Geological Society of London, Journal*, v. 156, p. 633–650.
- VITTORI, J., MORASH, A., SAVOYE, B., MARSSET, T., LOPEZ, M., DROZ, L., AND CREMER, M., 2000, The Quaternary Congo deep-sea fan: Preliminary results on reservoir complexity in turbiditic systems using 2D high resolution seismic and multibeam data: *Gulf Coast Section SEPM Foundation, 20th Annual Research Conference, Deep-Water Reservoirs of the World*, p. 1045–1058.
- WEIMER, P., AND LINK, M.H., eds., 1991, *Seismic Facies and Sedimentary Process of Submarine Fans and Turbidite Systems*: New York, Springer-Verlag, 447 p.
- WHIPPLE, K.X., 2004, Bedrock rivers and the geomorphology of active orogens: *Annual Review of Earth and Planetary Sciences*, v. 32, p. 151–185.
- WILLGOOSE, G., BRAS, R.L., AND RODRIGUEZ-ITURBE, I., 1991, A physical explanation of an observed link area–slope relationship: *Water Resources Research*, v. 27, p. 1697–1702.
- WINKER, C.D., AND BOOTH, J.R., 2000, Sedimentary dynamics of the salt-dominated continental slope, Gulf of Mexico: Integration of observations from the seafloor, near-surface, and deep subsurface: *Gulf Coast Section SEPM Foundation, 20th Annual Research Conference, Deep-Water Reservoirs of the World*, p. 1059–1086.
- WYNN, R.B., CRONIN, B.T., AND PEAKALL, J., 2007, Sinuous deep-water channels: Genesis, geometry and architecture: *Marine and Petroleum Geology*, v. 24, p. 341–387.
- YU, B., CANTELLI, A., MARR, J.G., PIRMEZ, C., O'BYRNE, C., AND PARKER, G., 2006, Experiments on self-channelized subaqueous fans emplaced by turbidity currents and dilute mudflows: *Journal of Sedimentary Research*, v. 76, p. 889–902.